

RESEARCH ARTICLE

Which Way In? The RalF Arf-GEF Orchestrates *Rickettsia* Host Cell Invasion

Kristen E. Rennoll-Bankert, M. Sayeedur Rahman, Joseph J. Gillespie, Mark L. Guillotte, Simran J. Kaur[‡], Stephanie S. Lehman, Magda Beier-Sexton, Abdu F. Azad*

Department of Microbiology and Immunology, University of Maryland School of Medicine, Baltimore, Maryland, United States of America

[‡] Current address: Fischell Department of Bioengineering, University of Maryland, College Park, Maryland, United States of America

* aazad@som.umaryland.edu



 OPEN ACCESS

Citation: Rennoll-Bankert KE, Rahman MS, Gillespie JJ, Guillotte ML, Kaur SJ, Lehman SS, et al. (2015) Which Way In? The RalF Arf-GEF Orchestrates *Rickettsia* Host Cell Invasion. *PLoS Pathog* 11(8): e1005115. doi:10.1371/journal.ppat.1005115

Editor: Isabelle Coppens, Johns Hopkins School of Public Health, UNITED STATES

Received: February 23, 2015

Accepted: July 28, 2015

Published: August 20, 2015

Copyright: © 2015 Rennoll-Bankert et al. This is an open access article distributed under the terms of the [Creative Commons Attribution License](https://creativecommons.org/licenses/by/4.0/), which permits unrestricted use, distribution, and reproduction in any medium, provided the original author and source are credited.

Data Availability Statement: All relevant data are within the paper and its Supporting Information files.

Funding: This work was supported with funds from the National Institute of Health/National Institute of Allergy and Infectious Diseases grants (R01AI017828, R01AI043006 and R01AI59118). KERB is supported in part by the NIH/NIAID T32AI095190 Signaling Pathways in Innate Immunity grant. The content is solely the responsibility of the authors and does not necessarily represent the official views of the funding agencies. The funders had no role in study design, data collection and

Abstract

Bacterial Sec7-domain-containing proteins (RalF) are known only from species of *Legionella* and *Rickettsia*, which have facultative and obligate intracellular lifestyles, respectively. *L. pneumophila* RalF, a type IV secretion system (T4SS) effector, is a guanine nucleotide exchange factor (GEF) of ADP-ribosylation factors (Arfs), activating and recruiting host Arf1 to the *Legionella*-containing vacuole. In contrast, previous *in vitro* studies showed *R. prowazekii* (Typhus Group) RalF is a functional Arf-GEF that localizes to the host plasma membrane and interacts with the actin cytoskeleton via a unique C-terminal domain. As RalF is differentially encoded across *Rickettsia* species (e.g., pseudogenized in all Spotted Fever Group species), it may function in lineage-specific biology and pathogenicity. Herein, we demonstrate RalF of *R. typhi* (Typhus Group) interacts with the *Rickettsia* T4SS coupling protein (RvhD4) via its proximal C-terminal sequence. RalF is expressed early during infection, with its inactivation via antibody blocking significantly reducing *R. typhi* host cell invasion. For *R. typhi* and *R. felis* (Transitional Group), RalF ectopic expression revealed subcellular localization with the host plasma membrane and actin cytoskeleton. Remarkably, *R. bellii* (Ancestral Group) RalF showed perinuclear localization reminiscent of ectopically expressed *Legionella* RalF, for which it shares several structural features. For *R. typhi*, RalF co-localization with Arf6 and PI(4,5)P₂ at entry foci on the host plasma membrane was determined to be critical for invasion. Thus, we propose recruitment of PI(4,5)P₂ at entry foci, mediated by RalF activation of Arf6, initiates actin remodeling and ultimately facilitates bacterial invasion. Collectively, our characterization of RalF as an invasin suggests that, despite carrying a similar Arf-GEF unknown from other bacteria, different intracellular lifestyles across *Rickettsia* and *Legionella* species have driven divergent roles for RalF during infection. Furthermore, our identification of lineage-specific Arf-GEF utilization across some rickettsial species illustrates different pathogenicity factors that define diverse agents of rickettsial diseases.

analysis, decision to publish, or preparation of the manuscript.

Competing Interests: The authors have declared that no competing interests exist.

Author Summary

Phylogenomics analysis indicates divergent mechanisms for host cell invasion across diverse species of obligate intracellular *Rickettsia*. For instance, only some *Rickettsia* species carry RalF, the rare bacterial Arf-GEF effector utilized by *Legionella pneumophila* to facilitate fusion of ER-derived membranes with its host-derived vacuole. For *R. prowazekii* (Typhus Group, TG), prior *in vitro* studies suggested the Arf-GEF activity of RalF, which is absent from Spotted Fever Group species, might be spatially regulated at the host plasma membrane. Herein, we demonstrate RalF of *R. typhi* (TG) and *R. felis* (Transitional Group) localizes to the host plasma membrane, yet *R. bellii* (Ancestral Group) RalF shows perinuclear localization reminiscent of RalF-mediated recruitment of Arf1 by *L. pneumophila* to its vacuole. For *R. typhi*, RalF expression occurs early during infection, with RalF inactivation significantly reducing host cell invasion. Furthermore, RalF co-localization with Arf6 and the phosphoinositide PI(4,5)P₂ at the host plasma membrane was determined to be critical for *R. typhi* invasion. Thus, our work illustrates that different intracellular lifestyles across species of *Rickettsia* and *Legionella* have driven divergent roles for RalF during host cell infection. Collectively, we identify lineage-specific Arf-GEF utilization across diverse rickettsial species, previously unappreciated mechanisms for host cell invasion and infection.

Introduction

Bacteria invading eukaryotic cells employ diverse strategies for successful entry, intracellular colonization and intercellular spread [1,2]. Whether facultative or obligate, intracellular species must either modify the phagocytic vacuole for survival or lyse the phagosome and live freely within the host cytoplasm (or invade other cellular organelles) [3–6]. Either strategy is delicately underpinned by bacterial secretion of effectors, which have a myriad of characterized functions: e.g., engaging host signaling pathways, rearranging the host cytoskeleton, polymerizing host actin, subverting host vesicular traffic, etc. [7–9]. It is well established that divergent effectors from distantly-related intracellular species can operate in similar processes [10]; e.g., actin nucleators from species of *Shigella*, *Listeria* and *Rickettsia* [11,12] and phospholipases from species of *Pseudomonas* and *Legionella* [13,14]. Conversely, the ability for highly similar effectors from distantly-related species to function differently in host cells is a phenomenon that is poorly known, probably reflective of effector repertoires being highly specific to bacterial genera [15–17].

Species of *Rickettsia* (*Alphaproteobacteria*: Rickettsiales) are Gram-negative obligate intracellular parasites of a wide range of eukaryotic species [18]. Rickettsiae bind to host cells and induce phagocytosis [19,20], with internalized bacteria released into the cytosol upon rapid escape from the phagocytic vacuole. Bacteria spread intercellularly upon death and lysis of host cells, though some species move intercellularly prior to host cell lysis via host actin polymerization [21–23]. Several surface proteins characterized for adhesion and/or entry of host cells (Sca5, Adr1, Adr2) [24–28] and activation of cytoskeletal vinculin (Sca4) [29] are conserved across sequenced *Rickettsia* genomes, as are several enzymes implicated in phagosomal lysis (TlyC, PLD, Pat1) [30–33]. In contrast, other characterized adhesins (Sca0, Sca1, Sca2) [34–38], proteins involved in Arp2/3-dependent (RickA) [39,40] and -independent (Sca2) [41,42] host actin polymerization, and another phospholipase (Pat2) [43,44] are sporadically encoded across rickettsial lineages. This suggests that, despite superficially similar infection strategies, diverse *Rickettsia* species employ distinct molecular mechanisms for successful colonization of host cells [45].

One such protein that is differentially encoded across *Rickettsia* genomes is a highly similar counterpart to the RalF protein of *Legionella* spp. Collectively, these proteins contain a Sec7-domain, which in eukaryotes functions as a guanine nucleotide exchange factor (GEF) of ADP-ribosylation factors (Arfs) [46]. Remarkably, bacterial Sec7-domain containing proteins are unknown from other bacteria [47]. *Legionella* RalF (RalF_L) is a secreted effector, with its proximal C-terminal sequence mediating secretion through the *dot/icm* type IV secretion system (T4SS) [48]. RalF_L activates and recruits host Arf1 to the *Legionella*-containing vacuole (LCV), which is a modification of the phagosome [49]. The structure of RalF_L contains two distinct domains: an N-terminal Sec7 domain (S7D) and a C-terminal Sec7-capping domain (SCD) that regulates active site access to Arfs [50]. The S7D and SCD across RalF_L and *Rickettsia* RalF (RalF_R) share ~45% aa identity, though an extended variable region flanks the SCD of RalF_R proteins at the C-terminus [51].

A comparative study of RalF_L and RalF_R determined similar GEF activities for both proteins, yet divergent subcellular localization patterns driven primarily by intrinsic characteristics of the SCD [52]. The RalF_L SCD positions the protein at the endoplasmic reticulum for interception of host secretory vesicles, while the RalF_R SCD targets the protein to the host plasma membrane. Furthermore, a proline-rich region within the extended variable region of RalF_R interacts with components of the host actin cytoskeleton. Subsequently, membrane sensor regions were identified within the SCDs of RalF_L and RalF_R, with differential enrichments in aromatic and positively charged residues determining divergent lipid substrates that regulate Arf-GEF activities [53]. Collectively, these studies suggest that these distinguishing features (divergent SCD sensor regions, RalF_R-specific cytoskeletal-binding domain) mediate the spatial regulation of RalF activity in two diverse intracellular species with very different lifestyles.

Despite tremendous insight on the possible function of RalF_R during rickettsial host cell infection, important questions are left unanswered. As previous studies were performed *in vitro* [52,53], it still remains unknown if those *Rickettsia* species that carry *ralF* genes actually express RalF_R during infection, and if so, at what time point. Furthermore, as GEFs confer the spatial regulation of different Arf classes at discrete cellular locales [54–57], the Arf(s) specificity of RalF_R needs to be determined in light of the different subcellular localization of the protein compared to *Legionella* spp. Our work presented here addresses these unknowns by demonstrating RalF expression by *R. typhi* early during host cell invasion. Across several *Rickettsia* species, we identified the domain requirements for positioning RalF at host membranes, and for *R. typhi*, determined that RalF co-localization with Arf6 and PI(4,5)P₂ at entry foci was critical for invasion. Altogether, our work identifies Arf-GEF utilization as a lineage-specific invasion mechanism, illuminating the variable strategies that drive *Rickettsia* infection of host cells.

Results

RalF_{Rt} interacts with the *rvh* T4SS coupling protein (RvhD4) via its proximal C-terminal sequence and is secreted during host cell infection

As predicted Arf-GEFs, we anticipated RalF_R proteins to be secreted extracellularly into the host cell. Prior to invasion, *L. pneumophila* utilizes its *dot/icm* I-T4SS to translocate RalF_L into host cells [48]. Like RalF_L, *R. typhi* RalF (RalF_{Rt}) lacks a predicted N-terminal Sec secretion signal [58], trans-membrane spanning regions [59] and a β-barrel structure [60], suggesting its secretion via a Sec-independent pathway, possibly the *Rickettsiales vir* homolog (*rvh*) T4SS [61]. Accordingly, in order to determine if RalF_{Rt} interacts with the *rvh* T4SS, we performed a bacterial two-hybrid assay with full length RalF_{Rt} (RalF_{RtFL}) and RvhD4, the *rvh* T4SS coupling protein. T4SS coupling proteins (VirD4 family) are ATPases that function as “gatekeepers” to regulate substrate entry into the T4SS channel [62,63]. Co-transformation of bait (encoding

RvhD4) and prey (encoding RalF_{RtFL}) plasmids in BacterioMatch II reporter electrocompetent cells resulted in bacterial growth on selective media (Fig 1A), indicating RalF_{RtFL} and RvhD4 interact, and thus implicating RalF_{Rt} as an *rvh* T4SS effector.

Secretion of RalF_L is dependent on hydrophobic residues within its C-terminal tail [48], while many other T4SS protein substrates have enrichments of positively charged residues at their C-termini that are important for secretion [64–66]. Accordingly, we evaluated RalF_{Rt} for the presence of a T4SS signal sequence (T4S) within its C-terminus. A T4S RalF_{Rt} truncation (RalF_{RtΔT4S}) was generated and tested for its ability to bind RvhD4 via the bacterial two-hybrid assay (Fig 1A). The percent growth of colony forming units (CFUs) of reporter cells harboring recombinant plasmids on dual selective screening medium was calculated relative to percent growth of CFUs obtained on non-selective His dropout medium by drop plate method for counting. An approximately 77% decrease in CFUs on dual selective media was observed with RalF_{RtΔT4S} compared to RalF_{RtFL}, indicating that the RalF C-terminus is important for interacting with RvhD4 (Fig 1B).

The ATPase activity of T4SS coupling proteins is essential for substrate translocation [67]. To confirm functionality of RvhD4, recombinant RvhD4 was assayed for ATPase activity. RvhD4 was found to release inorganic phosphate (Pi) from ATP in a concentration dependent manner compared to a rickettsial protein that lacks predicted ATPase activity (RT0600) (Fig 1C and 1D). This indicates *Rickettsia* RvhD4 is a functional ATPase that likely regulates protein secretion through the *rvh* T4SS.

The interaction of RalF_{Rt} with machinery of the *rvh* T4SS implies extracellular secretion. Our prior report that characterized the *R. typhi* surface proteome demonstrated that RalF_{Rt} is expressed and surface exposed [68]. To further confirm RalF_{Rt} secretion, purified *R. typhi* was treated with proteinase K, on the premise that surface exposed protein would be degraded with proteinase K treatment while subsurface proteins would be protected. Protease treatment caused a dose-dependent degradation of RalF_{Rt} with respect to the *R. typhi* cytoplasmic control protein, elongation factor Ts (EF-Ts, Fig 1E).

RalF_{Rt} is expressed early during infection and is required for *R. typhi* invasion of host cells

To determine when RalF_{Rt} is expressed during *R. typhi* infection, a polyclonal antibody against RalF_{Rt} was generated, qualified (S1 Fig) and used for immunofluorescence assays (Fig 1F). During early infection of host cells (10 min), RalF_{Rt} expression is high and diminishes as internalization progresses (30 min). Given RalF_{Rt} expression during early infection, we assessed its role during *R. typhi* invasion of host cells. When *R. typhi* was pre-treated with the anti-RalF_{Rt} polyclonal antibody, the average number of *R. typhi* per host cell decreased by 52% from an average of 10 to 4.8 bacteria per host cell (Fig 1G), indicating a role for RalF during host cell invasion. To rule out possible steric hindrance induced by the Fc portion of the anti-RalF_{Rt} antibody inhibiting rickettsial-host cell interactions that promote entry, *R. typhi* was pre-absorbed with anti-RalF_{Rt} Fab fragments. The average number of *R. typhi* per host cell was significantly decreased by 45% from 10 to 5.5 bacteria per host cell (Fig 1G) further confirming the involvement of RalF in host cell invasion.

RalF_R is divergent from RalF_L within the SCD lipid sensor region and also contains a C-terminal extension that is highly variable across *Rickettsia* homologs

Utilizing over 60 *Rickettsia* genome sequences, phylogenomics analyses were carried out to provide further insight on the role of RalF in rickettsial biology and pathogenesis. While a key

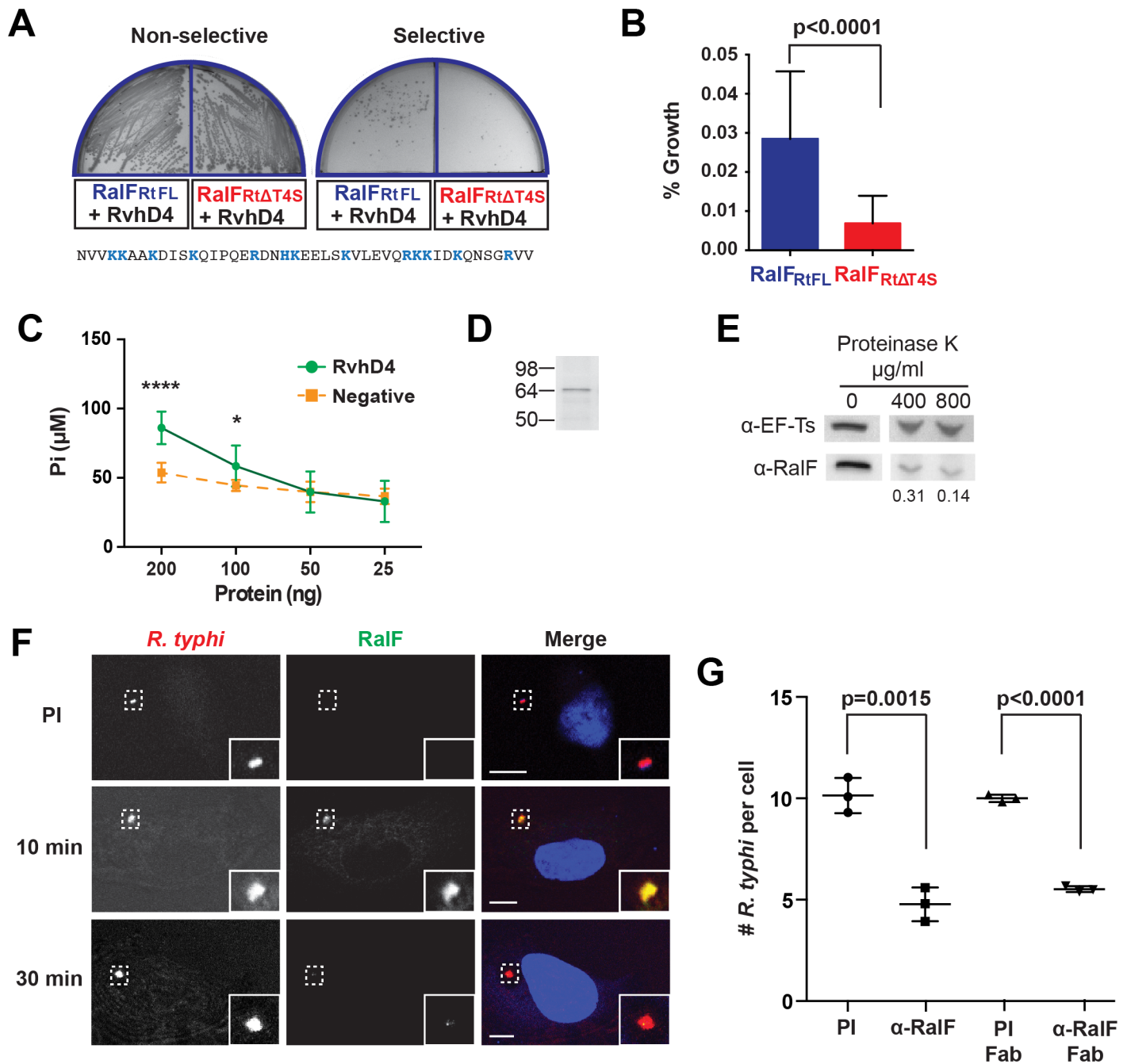


Fig 1. *R. typhi* RalF_{Rt} interacts with RvhD4 and is expressed early during host cell invasion. (A) Bacterial two-hybrid (B2H) assay reveals an interaction between RalF_{Rt} and RvhD4. *ralF_{Rt}FL* and *ralF_{Rt}ΔT4S* were cloned into pTRG (prey) and *rvhD4* was cloned into pBT (bait) of the B2H system. Constructed bait and prey plasmids were co-transformed into BacterioMatch II reporter electro-competent cells. Transformants were screened on non-selective plate (left) and positive interactions were identified on dual selective screening plate (right). The amino acid sequence deleted from *ralF_{Rt}ΔT4S* (positively charged residues are colored blue) is shown at bottom. (B) Quantification of bacterial growth in the B2H assay described in panel A. Percent growth of CFUs of reporter cells harboring recombinant plasmids on dual selective screening medium was calculated relative to CFUs obtained on non-selective medium. Error bars represent mean ± SD of three independent experiments (Student's two-sided t-test). (C) *R. typhi* RvhD4 exhibits ATPase activity. A series dilution of purified RvhD4 in assay buffer was incubated with reagent for 30 min at 21°C. The inorganic phosphate (Pi) released from ATP was quantified by measuring absorbance at OD 620 nm. As a negative control, a non-related *R. typhi* protein (RT0600) was assayed. Error bars represent mean ± SD of three independent experiments. * p = 0.01, **** p < 0.0001; Student's two-sided t-test. (D) Protein immunoblot of recombinant RvhD4 (~64 kDa) used in ATPase activity assays described in panel C. (E) RalF_{Rt} is surface exposed. Purified *R. typhi* was treated with 400 μg/mL or 800 μg/mL Proteinase K or in buffer alone for 1 hr. Lysates were resolved and immunoblotted for RalF or the *R. typhi* cytoplasmic control protein, elongation factor Ts (EF-Ts). Densitometry was performed using ImageJ and the intensity of RalF was normalized to EF-Ts. Representative image from two independent experiments is shown. Intensity of

RalF normalized to EF-Ts and relative to untreated control is shown below the immunoblots. (F) RalF is expressed during early infection. HeLa cells infected with *R. typhi* for 10 and 30 min were fixed and *R. typhi* and RalF detected with rat anti-*R. typhi* (red) and affinity purified rabbit anti-RalF_{Rt} (green) antibodies, respectively. DAPI (blue) is shown in the merged image. Boxed regions are enlarged to show detail. Pre-immune (PI) cells were treated with rabbit PI serum in place of anti-RalF_{Rt} antibody. (Scale bar: 10 μm). (G) Anti-RalF_{Rt} IgG and Fab fragments inhibit *R. typhi* host cell infection. HeLa cells were infected with partially purified *R. typhi* pre-absorbed for 30 min with 20 μg PI IgG serum, anti-RalF_{Rt} IgG, PI Fab fragments or anti-RalF_{Rt} Fab fragments. Cells were fixed 2 hrs post infection and *R. typhi* and the cell membrane detected with anti-*R. typhi* serum and Alexa Fluor 594 wheat germ agglutinin, respectively. The number of *R. typhi* per host cell was counted for 100 individual host cells in three independent experiments and normalized to PI serum. Error bars represent mean ± SD (Student's two-sided t-test).

doi:10.1371/journal.ppat.1005115.g001

factor in *R. typhi* infection of host cells, RalF-mediated invasion is not a strategy employed by all *Rickettsia* species, as evident by *ralF* pseudogenization in all species of Spotted Fever Group (SFG) rickettsiae, as well as two other species (*R. canadensis* and *R. helvetica*) [45]. Still, the remaining species, including *R. bellii* and all species within the Typhus Group (TG) and Transitional Group (TRG) rickettsiae, contain genes encoding RalF_R proteins that are highly conserved within the S7D and SCD as compared to RalF_L (Fig 2). Specifically, and in agreement with previous studies [52,53], all RalF_L and RalF_R proteins contain a highly conserved Sec7 active site within the S7D (S2A and S2B Fig), with RalF_R proteins having an enrichment of positively charged residues in the lipid sensor region of the SCD relative to RalF_L proteins (S3C Fig). Thus, based on these characteristics, all RalF_R proteins are predicted to spatially regulate their Arf-GEF activities at the host plasma membrane, where concentrated negatively charged phospholipids attract the RalF_R SCD [53].

Relative to RalF_L, the major distinguishing factor of RalF_R proteins is the presence of a variable sequence with Pro-rich region (VPR) within the C-terminal domain (Fig 2). Pro-rich regions are a common characteristic of proteins that target the actin cytoskeleton [70], and are typically present in Arf-GEFs recruited to cytoskeletal/plasma membrane junctions [71,72]. Across RalF_R proteins, the VPR is flanked by the SCD and T4S and is extraordinarily variable in sequence length and number of Pro residues across RalF_R proteins (Fig 2B). Remarkably, many SFG rickettsiae species, e.g. *R. montanensis*, contain putative ORFs encoding complete VPRs. Alignment of these ORFs with VPRs from full-length RalF_R proteins illustrates that a gene encoding RalF_R was present in the *Rickettsia* ancestor, with pseudogenization purging the complete Arf-GEF from most *Rickettsia* genomes (S4A Fig). This conclusion is supported by genome synteny analysis across *ralF_R* loci, which indicates a conserved position for *ralF* flanking the *maeB* gene in all sequenced *Rickettsia* genomes (S5A Fig). Thus, RalF_L and RalF_R proteins diversified early upon their establishment in ancestral *Legionella* and *Rickettsia* genomes, with the retention of VPRs within full-length RalF_R proteins implying an important function.

The RalF_R SCD regulates membrane localization while the VPR targets the host cytoskeleton

In light of the variability across the VPR of RalF_R proteins, we determined the C-terminal domain (CTD) requirements for subcellular localization across RalF_R proteins from several species (*R. typhi*, *R. felis*, *R. montanensis* and *R. bellii*) (Fig 3). The SCD- and VPR-mediated targeting to the host plasma membrane and actin cytoskeleton, respectively, for RalF of *R. prowazekii* (RalF_{Rp}) was used as a reference [52,53]. *R. typhi* and *R. felis* full-length RalF (RalF_{FL}) proteins primarily had diffuse staining within the cytoplasm with some plasma membrane localization. However, RalF_{CTD} (SCD-VPR-T4S) localized strongly to the plasma membrane and disrupted actin stress fibers. Additionally, *R. typhi* and *R. felis* RalF_{CTD} induced membrane ruffling and microvilli-like protrusions suggesting that the CTD plays a role in cytoskeletal rearrangements, similar to the known Arf6-GEF, EFA6 [71,72]. Furthermore, RalF_{VPR} (VPR-T4S), as well as the full-length VPR-containing ORF of *R. montanensis*, did not

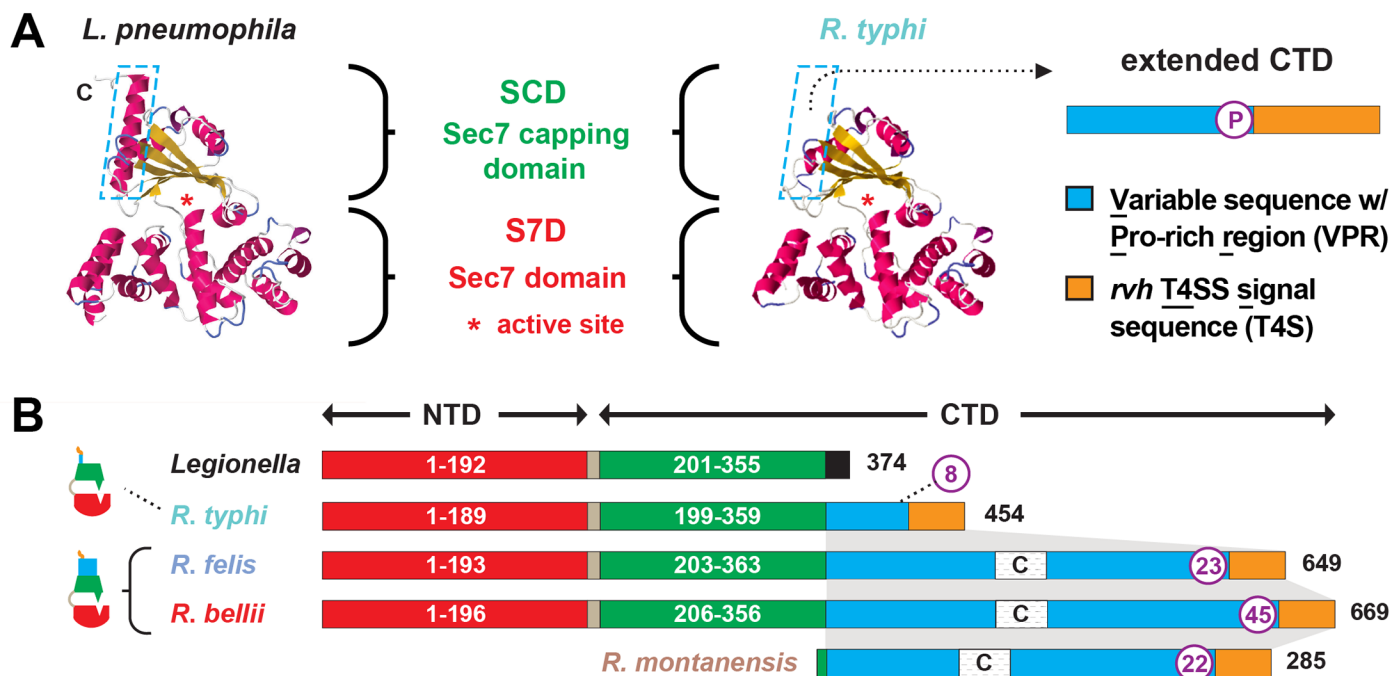


Fig 2. Characteristics and comparative analysis of bacterial Sec7 domain-containing proteins (RalF). (A) Comparison of the crystal structure of *Legionella pneumophila* RalF (PDB 4C7P) [53] with the predicted structure of *R. typhi* RalF (RT0362). Modeling done with Phyre2 [69]. The delineation of the Sec7 domain (S7D, red) and Sec7-capping domain (SCD, green) is shown, with an approximation of the active site Glu (asterisk), which is essential for Arf recruitment to the *Legionella* containing vacuole [52]. The distinguishing feature of the otherwise highly similar proteins is the extended C-terminal domain in *R. typhi* RalF relative to *L. pneumophila* RalF. The blue dashed box depicts the extended C-terminal domain of *Rickettsia* RalF sequences, which can be delineated into a variable sequence with Pro-rich region (VPR) and an *rvh* T4SS signal sequence (T4S). (B) Domain organization of *Legionella* and *Rickettsia* RalF proteins. The structural conservation witnessed in panel A is encoded by conserved S7D (S2B Fig) and SCD (S3B Fig) sequences (~45% ID across *Legionella* and *Rickettsia*). *Rickettsia* RalF VPRs vary extensively across homologs; some *Rickettsia* RalF proteins contain only the VPR and T4S (S4A Fig). C, coiled-coil. Number of Pro residues within purple circles. NCBI GenBank accession numbers for all proteins are provided in the legend of S2 Fig.

doi:10.1371/journal.ppat.1005115.g002

uniformly localize to the host plasma membrane, but instead were found strongly associated with intact actin stress fibers. Collectively, these results indicate that *R. typhi* and *R. felis* RalF proteins are similar to RalF_{RP}, with both the SCD and VPR required to spatially regulate Arf-GEF activities at plasma membrane/actin cytoskeletal junctions.

Remarkably, RalF_{FL} and RalF_{CTD} of *R. bellii* did not target the plasma membrane, yet instead showed perinuclear localization reminiscent of ectopically expressed RalF_L. As *R. bellii* RalF_{VPR} associated with intact actin stress fibers, these data collectively indicate that the SCD alone is sufficient to localize RalF_{RB} to the host cytoplasm. Visualization of the SCD sequence alignment across all RalF_L and RalF_R proteins revealed that RalF_{RB} lacks three separate insertions within the SCD that are conserved in all other RalF_R proteins (S3B Fig). Thus, from a structural perspective, the SCD of RalF_{RB} is more similar to RalF_L proteins than RalF_R proteins, which could explain why the SCD of *R. bellii* localizes to the perinuclear region of the cytoplasm. This is consistent with *R. bellii* sharing more genomic attributes with *Legionella* spp. [73], as well as being able to grow in various amoeba species unlike most other *Rickettsia* spp. (see Discussion).

RalF membrane localization was further confirmed using two independent approaches. First, membrane fractionation of HeLa cells transfected with RalF-expressing plasmids revealed that all RalF_{CTD} proteins were predominately enriched in the membrane fraction, with RalF_{FL} and RalF_{VPR} proteins having less membrane enrichment (Fig 3 and S6 Fig). Second, RalF transfected cells were stained with Alexa Fluor 594 wheat germ agglutinin to detect plasma

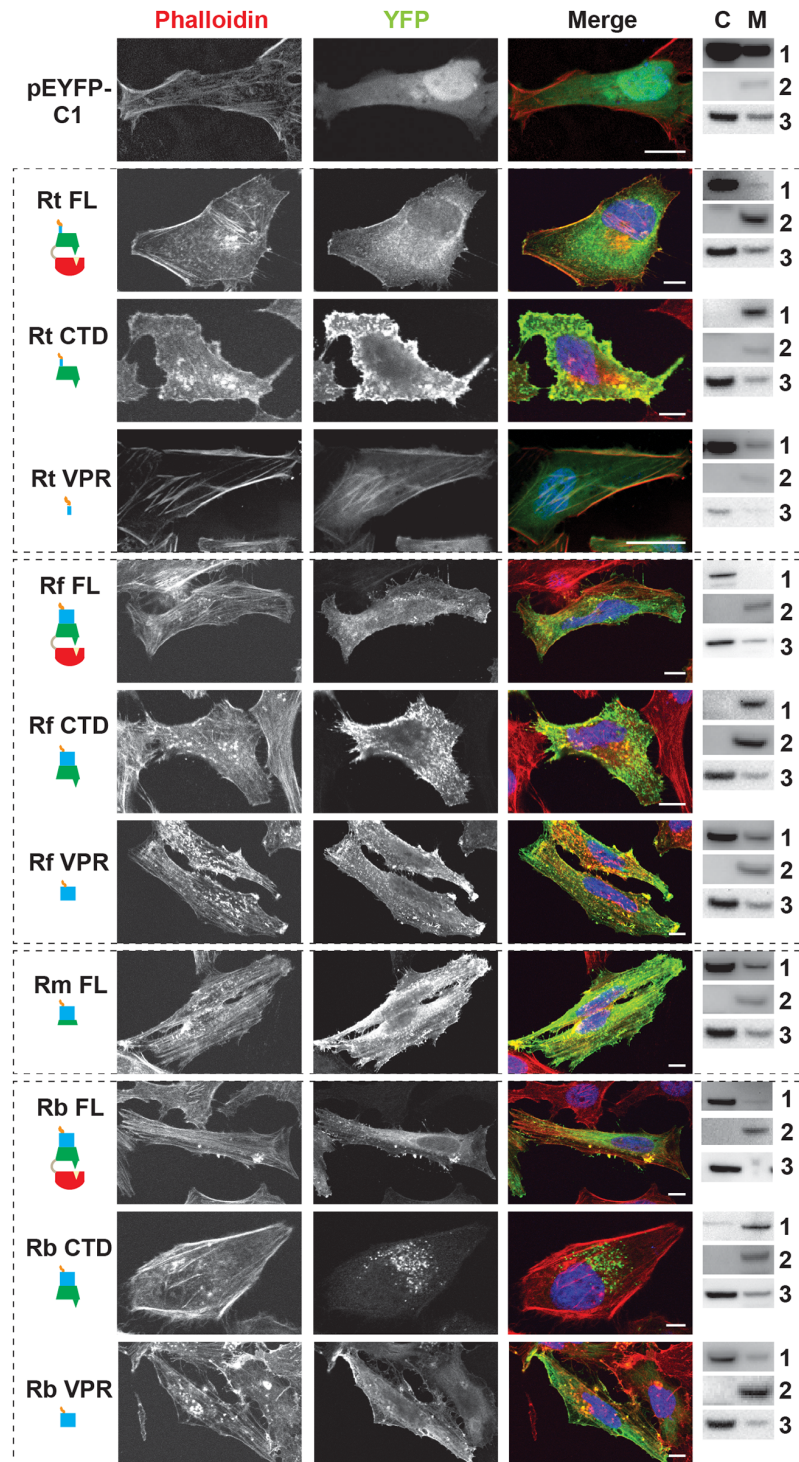


Fig 3. RalF subcellular localization and actin filament disruption mediated by the SCD and VPR. HeLa cells transfected with YFP tagged constructs (green, described in Fig 2B) were stained with Alexa Fluor 594 phalloidin to detect actin (red). DAPI (blue) is shown in the merged image. Cytoplasmic (C) and membrane (M) localization was confirmed via membrane fractionation of HEK293T cells Lipofectamine 2000 transfected with the indicated plasmids followed by immunoblotting. Immunoblot primary antibodies: 1, rabbit anti-GFP (Life Technologies); 2, membrane marker rabbit anti-Calnexin (Abcam); 3, cytoplasmic marker mouse anti-GAPDH (Abcam). Rt, *R. typhi*; Rf, *R. felis*; Rm, *R. montanensis*; Rb, *R. bellii*. (Scale bar: 10 μ m).

doi:10.1371/journal.ppat.1005115.g003

membrane or probed with anti-PDI (endoplasmic reticulum) or anti-GM130 (Golgi apparatus) antibodies (Fig 4 and S7 Fig), with the Pearson's correlation coefficients calculated to measure co-localization with the respective membrane markers (S8 Fig). RalF_{CTD} of *R. typhi*, *R. felis*, *R. montanensis* indicate localization to the plasma membrane, while *R. bellii* RalF_{CTD} localized to the endoplasmic reticulum membrane recapitulating results observed with labeling host cell actin (Fig 3). Collectively, these data demonstrate the affinities of RalF_R proteins for host membranes, identifying the SCD as the major determinant for membrane localization, combined with the targeting of actin cytoskeleton by the VPR (Table 1).

Finally, for *R. typhi*, we monitored the subcellular localization of its RalF_{CTD} construct lacking the T4S (RalF_{RiCTDΔT4S}). We observed indistinguishable localization patterns between RalF_{RiCTD} and RalF_{RiCTDΔT4S} (S4C Fig), suggesting that the T4S has no effect on localization or stress fiber disruption. In conjunction with results above (Fig 1A and 1B), these data bolster the role of the T4S of RalF_R proteins as an *rvh* T4SS translocation signal.

Plasma membrane localization of RalF_{Rt} is dependent on PI(4,5)P₂

Previous studies showed the SCD of RalF_{Rp} has affinities for negatively-charged phospholipids; i.e., phosphatidylinositol 4,5-bisphosphate (PI(4,5)P₂) and phosphatidylinositol 3,4,5-trisphosphate (PI(3,4,5)P₃) [52,53]. Given the enrichment of PI(4,5)P₂ at host membranes during early stages of phagocytosis [74], we evaluated the role of PI(4,5)P₂ in RalF_R localization. As a baseline, we utilized the standard phospholipase C (PLC)-mediated catalyzation of PI(4,5)P₂ within the IP3/DAG pathway of host cells [75]. Specifically, in the presence of ionomycin and Ca²⁺, PI(4,5)P₂ is hydrolyzed to inositol 1,4,5-trisphosphate and diacylglycerol via PLC isozymes that regularly deplete the plasma membrane of PI(4,5)P₂ following its role as a substrate in many signaling pathways [76]. To test PI(4,5)P₂-dependent localization of RalF_{Rt} to the plasma membrane, HeLa cells ectopically expressing RalF_{RiCTD} were treated with ionomycin and Ca²⁺, with the distribution pattern of RalF_{RiCTD} monitored by immunofluorescence. With ionomycin and Ca²⁺ treatment, RalF_{RiCTD} becomes cytosolic compared to plasma membrane localization in the presence of ionomycin alone (Fig 5A). Upon treatment with EGTA, which chelates Ca²⁺, PI(4,5)P₂ accumulates and RalF_{RiCTD} returns to the plasma membrane. HeLa cells expressing GFP-C1-PLCδ-PH, a biosensor of PI(4,5)P₂, were used as a positive control to demonstrate the hydrolysis of PI(4,5)P₂ in the presence of ionomycin and Ca²⁺. Additionally, RalF_{RbCTD} subcellular localization was shown to be unaffected by PI(4,5)P₂ hydrolysis, consistent with its perinuclear distribution in host cells. Collectively, these data indicate that PI(4,5)P₂ enrichment at the host plasma membrane is a requirement for efficient recruitment of RalF_{Rt}, and probably also RalF_{Rf}, given its similar subcellular localization pattern.

PI(4,5)P₂ recruitment is critical for *R. typhi* invasion of host cells

Phosphatidylinositols enriched at the host plasma membrane often play a critical role in bacterial internalization [74]. Given that RalF_{Rt} is expressed early (Fig 1F) and required (Fig 1G) for host invasion, and its localization to the host plasma membrane requires PI(4,5)P₂ enrichment (Fig 5A), we sought to determine if PI(4,5)P₂ is recruited by RalF_{Rt} during *R. typhi* infection. PI(4,5)P₂ localization during *R. typhi* invasion was analyzed using immunofluorescence microscopy with GFP-C1-PLCδ-PH as a biosensor of PI(4,5)P₂ localization. During early infection (i.e. 5 and 10 min post infection), PI(4,5)P₂ was highly localized to pseudopodia at the *R. typhi* entry foci (Fig 5B). As internalization progressed, *R. typhi* was surrounded by a vacuole with diminished PI(4,5)P₂ localization. Once *R. typhi* detached from the membrane, it was no longer associated with PI(4,5)P₂. Furthermore, detection of RalF_{Rt} during the infection process revealed co-localization of PI(4,5)P₂ and RalF_{Rt} during early infection (Fig 5C). In agreement

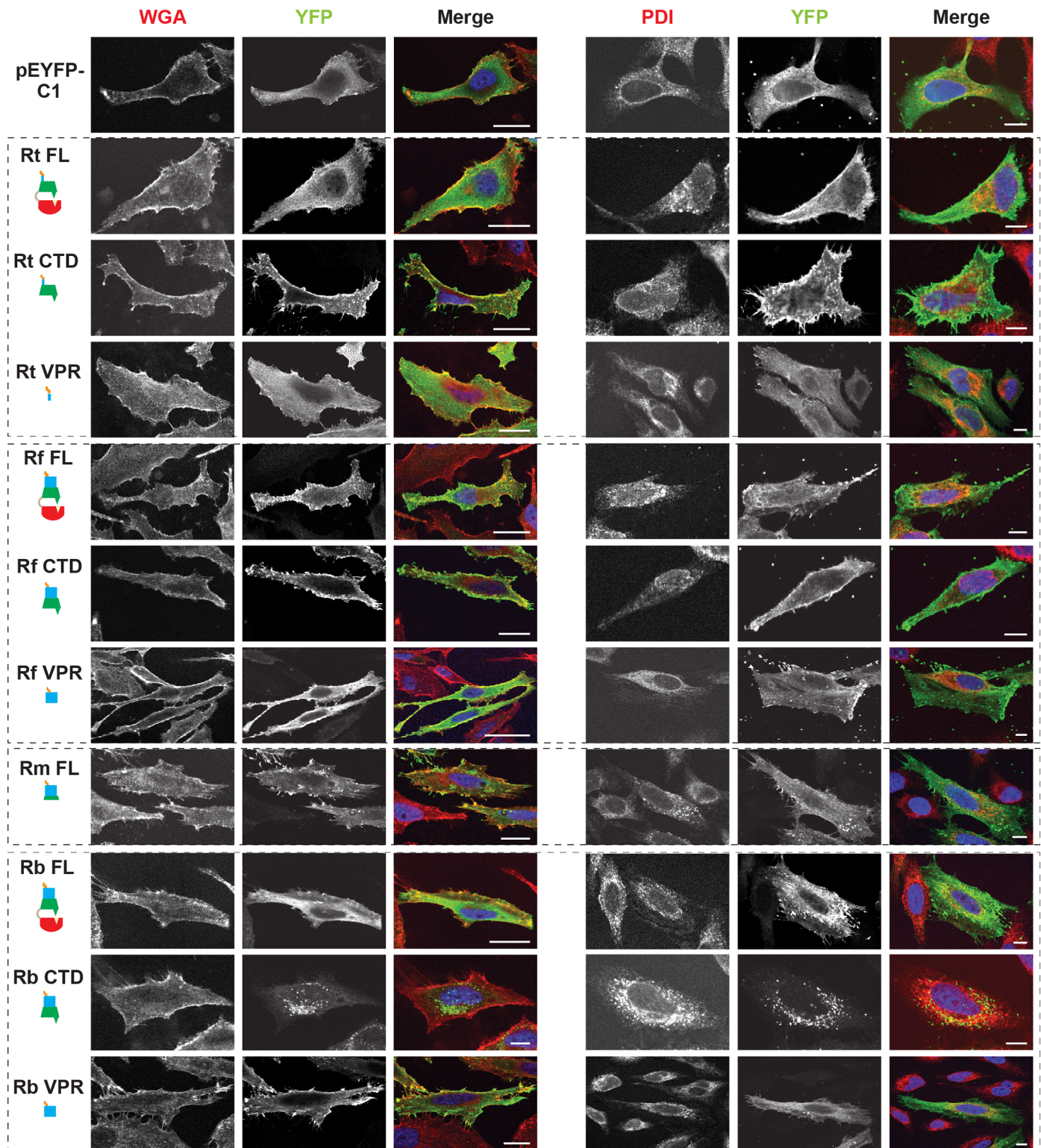


Fig 4. Subcellular localization of rickettsial RalF proteins to host membranes. HeLa cells expressing YFP tagged RalF proteins (green, described in Fig 2) were fixed and stained with Alexa Fluor 594 wheat germ agglutinin (WGA) to detect the plasma membrane (left) or anti-PDI antibody to detect the endoplasmic reticulum (right). DAPI (blue) is shown in the merged image. (Scale bar: 10 μ m).

doi:10.1371/journal.ppat.1005115.g004

Table 1. *Rickettsia* RalF domain characterization.

	Plasma Membrane Localization ^a	Perinuclear Localization ^a	Actin Binding ^a	Stress Fibers ^b	Membrane Ruffles ^b
Rt FL	+	-	+	+	-
Rt CTD	+	-	+	-	+
Rt VPR	-	-	+	+	-
Rf FL	+	-	+	+	-
Rf CTD	+	-	+	-	+
Rf VPR	-	-	+	+	-
Rm FL	-	-	+	+	-
Rb FL	-	+	+	+	-
Rb CTD	-	+	-	+	-
Rb VPR	-	-	+	+	-

Summary of protein localization, actin binding, stress fiber disruption and membrane ruffle formation for each RalF protein based on immunofluorescence and densitometry data (Figs 3, 4, and S6, S7 and S8 Figs).

^a +; association, -; negligible association

^b +; present, -; absent

doi:10.1371/journal.ppat.1005115.t001

with RalF_{Rt} early expression, which diminished at later stages of infection (Fig 1F), PI(4,5)P₂ recruitment decreased as infection progressed.

Finally, we evaluated whether or not the recruitment of PI(4,5)P₂ to *R. typhi* entry foci is critical for *R. typhi* infection. Pretreatment of HeLa cells with ionomycin and Ca²⁺ to deplete PI(4,5)P₂ from the membrane prior to infection resulted in a significant decrease in *R. typhi* infection (Fig 5D), strengthening the evidence that PI(4,5)P₂ is a target molecule involved in RalF_{Rt}-associated host cell invasion.

RalF_{Rt} interacts with Arf6 but not Arf5

The Arf-GEF activity of RalF_L is activated upon membrane binding, with Arf1 the preferred substrate [49,52]. Arf1 is predominantly localized to the Golgi apparatus and plays a role in intra-Golgi transport [77]. Given the association of RalF_{Rt} with the plasma membrane, we hypothesized that it might instead recruit Arf6, which is predominantly localized to the plasma membrane where it is involved in endocytosis, endosomal recycling and exocytosis of secretory granules [78–81]. Using immunofluorescence, RalF_{RtFL} was found to recruit Arf6 but neither Arf5 (Fig 6A) nor Arf1 (S9 Fig) to the plasma membrane. Arf5 localizes primarily to the endoplasmic reticulum/Golgi intermediate compartment and the cis-Golgi, where it regulates endoplasmic reticulum to Golgi transport; therefore, Arf5 was used as a negative control [82]. Interestingly, RalF_{RbFL} was similarly found to co-localize with Arf6 but not Arf5 or Arf1 in the perinuclear space.

To further confirm a RalF_{RtFL} and Arf6 interaction, a protein pull-down assay was performed. Using rHis-RalF_{RtFL} as bait and mRFP-Arf5 or mRFP-Arf6 as the prey, we confirmed that RalF_{RtFL} interacted with Arf6 and not Arf5 (Fig 6B).

Arf6 recruitment is critical for *R. typhi* invasion of host cells

Activation of Arf6 at the plasma membrane drives the recruitment of phospholipase D and phosphatidylinositol 4-phosphate 5-kinase (PIP5K), which ultimately results in actin remodeling [83,84]. To determine if Arf6 is recruited during *R. typhi* entry, we used immunofluorescence microscopy to monitor Arf6 localization. As early as 10 min post infection, Arf6 was

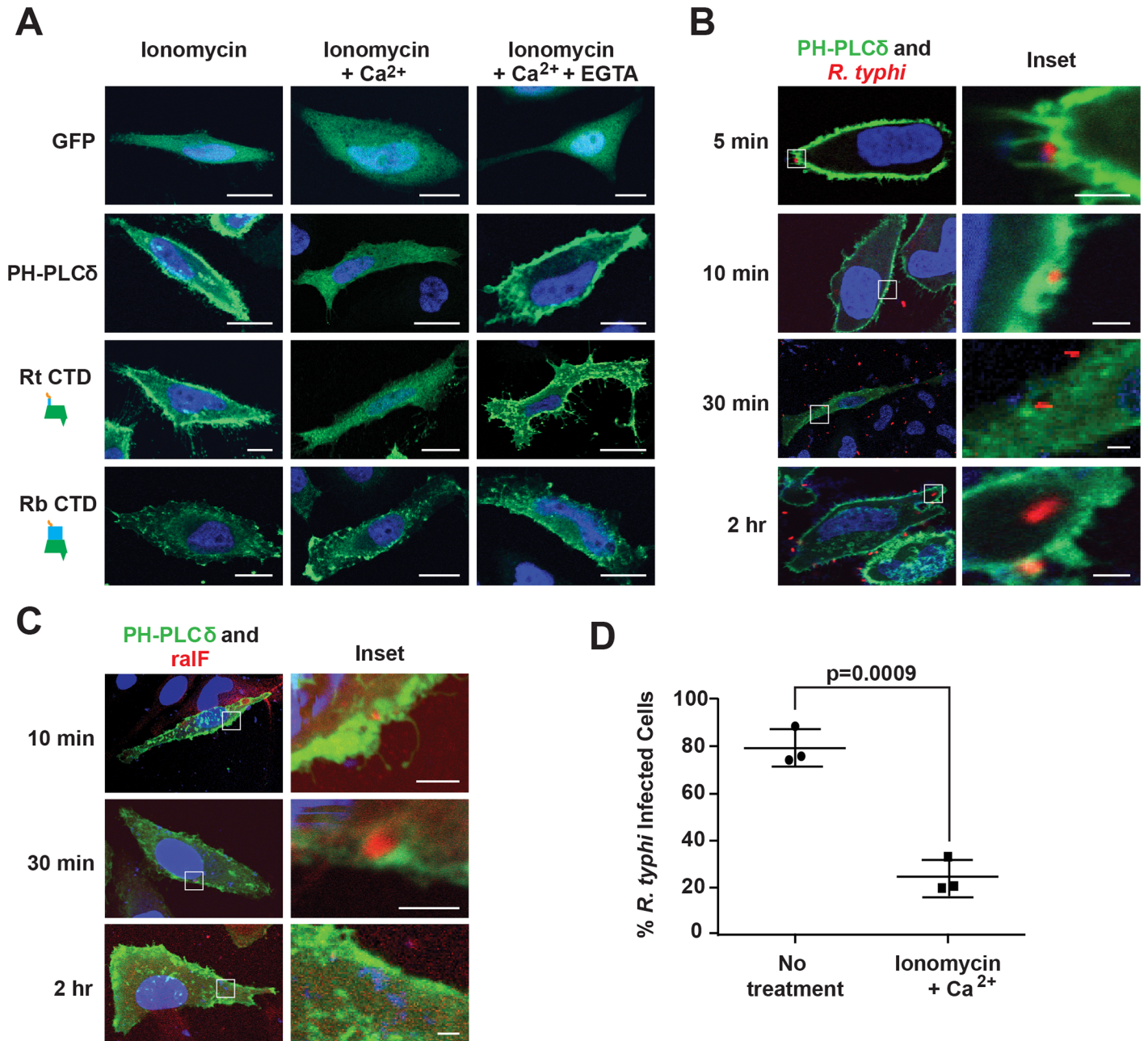


Fig 5. PI(4,5)P₂ interacts with RalF_{Rt} and mediates *R. typhi* infection. (A) RalF_{RtCTD} co-localizes with PI(4,5)P₂. HeLa cells transfected with pEYFP-C1 empty vector, GFP-C1-PLCδ-PH (a PI(4,5)P₂ biosensor), EYFP-RalF_{RtCTD}, or EYFP-RalF_{RbCTD} were treated with 5 μM ionomycin alone, with Ca²⁺, or with Ca²⁺ and EGTA. Nuclei were stained with DAPI (blue). (Scale bar: 10 μm). (B) PI(4,5)P₂ is recruited during *R. typhi* infection. HeLa cells transfected with GFP-C1-PLCδ-PH (green) were infected with *R. typhi* (MOI ~100:1) for indicated times. *R. typhi* was detected with rat anti-*R. typhi* serum and Alexa Fluor 594 anti-rat antibody (red). Nuclei were stained with DAPI (blue). Boxed regions are enlarged to show detail (inset). (Scale bar: 1 μm). (C) RalF localizes to PI(4,5)P₂-enriched regions of the plasma membrane during *R. typhi* infection. HeLa cells transfected with GFP-C1-PLCδ-PH (green) were infected with *R. typhi* (MOI ~100:1) for indicated times. RalF_{Rt} was detected with rabbit anti-RalF_{Rt} and Alexa Fluor 594 anti-rabbit antibodies (red). Nuclei were stained with DAPI (blue). Boxed regions are enlarged to show detail (inset). (Scale bar: 1 μm). (D) Ionomycin and Ca²⁺ treatment decreases *R. typhi* infection. HeLa cells treated with 5 μM ionomycin and Ca²⁺ or no treatment were infected with *R. typhi* (MOI ~100:1) for 2 hrs. *R. typhi* was detected with rat anti-*R. typhi* serum and Alexa Fluor 488 anti-rat antibody. Cell membrane was stained with Alexa Fluor 594 wheat germ agglutinin. The number of infected host cells was counted, with percent infection of three independent experiments (100 host cells counted for each) plotted. Error bars represent mean ± SD (Student's two-sided t-test).

doi:10.1371/journal.ppat.1005115.g005

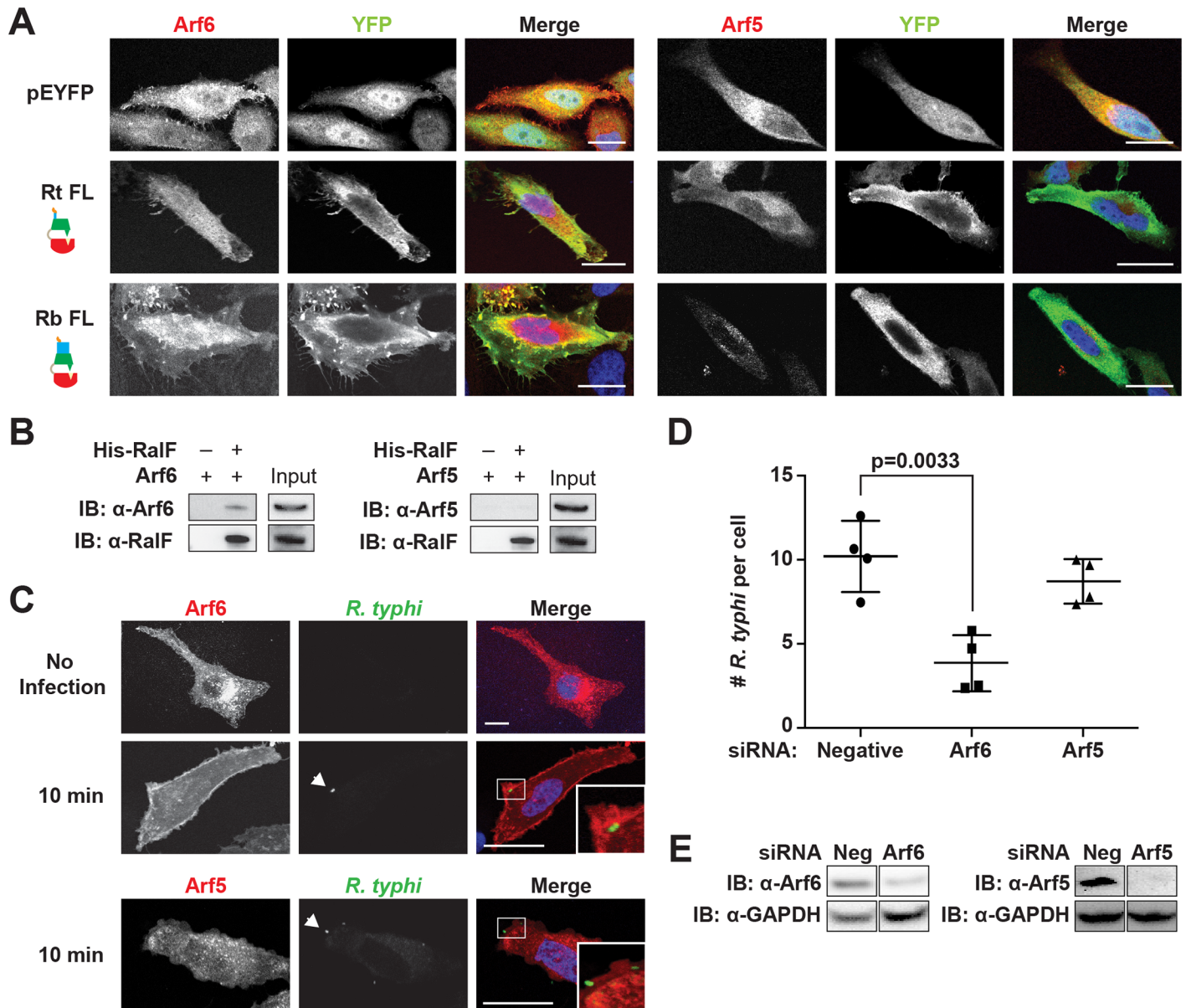


Fig 6. Arf6 is recruited by *R. typhi* RalF and is required for infection. (A) Ectopically expressed RalF_{RtFL} co-localizes with Arf6 but not Arf5. HeLa cells co-expressing EYFP, EYFP-RalF_{RtFL} or EYFP-RalF_{RbFL} and mRFP-Arf6 (left) or -Arf5 (right) were fixed with 4% para-formaldehyde. Nuclei were stained with DAPI (blue). (Scale bar: 10 μ m). (B) RalF_{RtFL} pull-down of Arf6. Lysates from HEK293T cells expressing mRFP-Arf5 or -Arf6 were incubated with HisPur Cobalt resin bound with rHis-RalF_{RtFL} or resin alone. Bound proteins were eluted with imidazole and analyzed by protein immunoblot using antibodies as indicated. (C) Arf6 is recruited during *R. typhi* entry. HeLa cells expressing mRFP-Arf5 or -Arf6 (red) were infected with partially purified *R. typhi* (MOI ~100). Ten minutes post infection, cells were fixed and *R. typhi* detected with anti-*R. typhi* serum (green). DAPI (blue) is shown in the merged image. Boxed regions are enlarged to show detail. White arrowheads indicate *R. typhi*. (Scale bar: 5 μ m). (D) Arf6 knockdown inhibits *R. typhi* infection. HeLa cells transfected with negative, Arf6, or Arf5 siRNA were infected with partially purified *R. typhi* (MOI ~100). At 2 hrs post infection, cells were fixed, plasma membrane stained with Alexa Fluor 594 wheat germ agglutinin, and *R. typhi* detected with rat anti-*R. typhi* serum and Alexa Fluor 488 anti-rat antibody. The number of *R. typhi* per host cell was counted for 100 host cells for three independent experiments. Error bars represent mean \pm SD (Student's two-sided t-test). (Scale bar: 5 μ m). (E) Confirmation of Arf6 and Arf5 knockdown. Arf6 and Arf5 knockdown, 80% and 96% respectively, was confirmed by western blot and densitometry analysis using ImageJ (NIH).

doi:10.1371/journal.ppat.1005115.g006

recruited to the plasma membrane at *R. typhi* entry foci, while Arf5 remained cytoplasmic (Fig 6C). Given that RalF_{Rt} localizes with Arf6 at plasma membrane (Fig 6A) and recruits Arf6 at the *R. typhi* entry foci (Fig 6C), we predicted that knockdown of Arf6 would decrease *R. typhi* infection. Indeed, siRNA-mediated Arf6 knockdown significantly decreased the number of *R. typhi* per cell, while Arf5 knockdown had no significant effect on *R. typhi* infection (Fig 6D and 6E). These results indicate that RalF_{Rt} recruits Arf6 at the plasma membrane during early infection, with spatially regulated Arf-GEF activity required for host cell invasion.

Discussion

Bacteria invading eukaryotic cells employ diverse strategies to subvert the host cellular actin cytoskeleton, allowing for internalization into normally non-phagocytic host cells [85]. For some bacterial species, surface proteins bind host cell receptors and trigger an “outside-in” signaling cascade, which induces cytoskeletal rearrangements and recruits the endocytic machinery to entry foci [86]. Such receptor-mediated induction of bacterial uptake is a strategy employed by *Listeria monocytogenes*, which utilizes two adhesins (InlA and InlB) to bind host proteins (E-cadherin, receptor gC1qR, proteoglycans) and activate the tyrosine kinase receptor Met [87]. Invasive species of *Yersinia* also employ two adhesins (invasin and YadA) to bind a subset of β 1-integrin host receptors, facilitating invasion that is dependent on signaling from the Rho GTPase Rac1 and activation of the actin nucleating complex Arp2/3 [88,89]. Alternatively, other bacterial species translocate effectors into host cells to initiate actin remodeling and facilitate bacterial uptake. For example, *Salmonella typhimurium* utilizes its type III secretion system to inject host cells with the effector SopE, which stimulates GDP/GTP nucleotide exchange on Rho GTPases Rac1 and Cdc42, resulting in membrane ruffling and actin cytoskeleton rearrangement [90]. While a receptor-mediated process has been previously characterized for *R. conorii* invasion of mammalian cells (discussed below), to date no secreted effectors for any *Rickettsia* species have been characterized for their role in inducing uptake into host cells.

While most species of the order Rickettsiales encode the *rvh* T4SS [91], effectors have only been identified for some species of the family Anaplasmataceae. For *Anaplasma phagocytophilum*, *rvh* effectors are translocated to the mitochondria (Ats-1) and nucleus (AnkA) to inhibit etoposide-induced apoptosis and down-regulate host defense genes, respectively [92–94]. AM185, AM470, AM705 (AnkA), and AM1141 have been identified as putative *rvh* T4SS effectors of *Anaplasma marginale* using a heterologous T4SS (*L. pneumophila dot/icm*), yet none have been characterized for their roles in invasion [95]. *Ehrlichia chaffeensis* utilizes the *rvh* T4SS to translocate the effector ECH0825 into host mitochondria, resulting in inhibition of Bax-induced apoptosis [96]. Herein, we identified RalF as the first *rvh* T4SS effector for species in the family Rickettsiaceae. We provide evidence that *R. typhi* RalF interacts with RvhD4, the *rvh* T4SS coupling protein that presumably recognizes effectors and regulates their translocation similar to VirD4 proteins of other P-type T4SSs. Treatment of purified *R. typhi* with proteinase K degraded surface exposed RalF, providing further evidence that RalF is secreted. Furthermore, using immunofluorescence we show that RalF_{Rt} is expressed early during host cell invasion. Because RalF is expressed early during invasion, we hypothesized that RalF is critical for invasion, which was confirmed using antibody pretreatment assays.

Prior studies comparing the subcellular localization of ectopic RalF_L and RalF_{Rp} determined that, despite strong conservation in the S7D and SCD across these proteins, cryptic signatures within the SCD targeted these proteins to different host membranes [52,53]. RalF_{Rp} localization to the plasma membrane, mediated by elevated positively charged residues within the lipid sensor of the SCD, was anticipated to be true for other RalF_R proteins, given the strong sequence conservation within the SCD across RalF_R homologs. Furthermore, despite extensive

variation within the VPR across RalF_R proteins, the presence of proline-rich regions in all proteins suggested that this region likely encodes a conserved motif that facilitates interaction with the host cytoskeleton, as was shown for RalF_{RP} [52,53]. Indeed, our co-localization assays confirmed that, for RalF of *R. typhi* and *R. felis*, the SCD mediates interaction with the host plasma membrane, with the VPR facilitating interaction with the host cytoskeleton.

In contrast, the perinuclear localization of RalF of *R. bellii*, reminiscent of the localization of ectopic expressed RalF_L proteins at the host secretory network, was unexpected. The VPR of RalF_{Rb} is similar in length to VPRs of RalF proteins from *R. felis*, *R. akari* and *R. australis*, with all of these proteins predicted to encode a coiled-coil motif typical of some eukaryotic Arf-GEFs; e.g., EFA6 [71]. While containing an extraordinary number of Pro residues, the VPR of RalF_{Rb} nonetheless targets the host cytoskeleton, suggesting that other characteristics of the protein mediate its localization to the cytoplasm. Indeed, *in silico* analyses revealed three conserved insertions within the SCD of RalF_R proteins that are absent from RalF_{Rb}. Furthermore, relative to all RalF proteins, the S7D of RalF_{Rb} contains an odd insertion as well as a slightly less hydrophobic active site (S2 Fig), the significance of which is unknown. It is tempting to speculate that the perinuclear localization of RalF_{Rb} reflects a unique cytosolic lifestyle of *R. bellii*, an ancestral lineage with a different genomic repertoire relative to other *Rickettsia* species [51] and the unique ability to grow and survive in several species of amoeba [73]. As *R. bellii* has been observed invading nuclei of mammalian cells *in vitro* [73], RalF may play a role in this process, though other *Rickettsia* species that lack RalF also are known to invade host cell nuclei [97]. Notwithstanding, the SCD-driven perinuclear localization of RalF_{Rb} might thus be considered the retention of an ancestral role for RalF_R proteins in targeting host vesicular trafficking, similar to RalF_L proteins. Collectively, our detailed dissection of the domain requirements for subcellular localization strongly implies differential utilization of Arf-GEF activities for those species of *Rickettsia* that encode RalF.

RalF_{Rb} aside, the subcellular localization of other RalF_R proteins to the plasma membrane suggested Arf6 might be their preferred host target, given the predominant localization of Arf6 to the plasma membrane [98] and a previous study showing that RalF_{RP} can catalyze nucleotide exchange on Arf6 [52]. Arf6 activation by some intracellular pathogens (e.g., species of *Salmonella*, *Yersinia* and *Chlamydia*) is known to induce actin remodeling and mediate bacterial invasion via unique pathways. *Salmonella enterica* activates Arf6 to recruit the Arf-GEF ARNO, which in turn activates Arf1 to enable WASP family veroprolin homolog (WAVE) regulatory complex-dependent actin assembly [99]. Arf6 activation by species of *Yersinia* and *Chlamydia* leads to activated PIP5K, which converts PI(4)P to PI(4,5)P₂ at the plasma membrane [100,101]. As PI(4,5)P₂ enrichment at the host plasma membrane modulates many actin-binding proteins, including α -actinin, talin, vinculin, gelsolin, and the WASP-Arp2/3 complex [102–107], effector-driven accumulation of this phosphatidylinositol can be considered a strategy for induction of phagocytosis.

Given that *R. typhi* secretes RalF early during host cell invasion, we hypothesized that this Arf-GEF recruits Arf6 to entry foci, precipitating the enrichment of PI(4,5)P₂ at the plasma membrane to facilitate bacterial invasion. Indeed, our *in vitro* and *in vivo* results confirm that Arf6 co-localizes with RalF and *R. typhi* at entry foci. Additionally, during *R. typhi* infection, PI(4,5)P₂ noticeably accumulated in the membranes of pseudopodia, with a decreased concentration at the base of the phagocytic cup as internalization progressed. Furthermore, the role of PI(4,5)P₂ in bacterial internalization was bolstered by the significant reduction in *R. typhi* invasion upon PI(4,5)P₂ hydrolysis. Thus, an increase in PI(4,5)P₂ induced by rickettsial RalF activation of Arf6 is predicted to initiate actin remodeling and ultimately facilitate bacterial invasion (Fig 7). Remarkably, this function for RalF_R is markedly different than RalF_L, which is utilized by *L. pneumophila* to recruit Arf1 to the LCV [49]. Unlike species of *Legionella*,

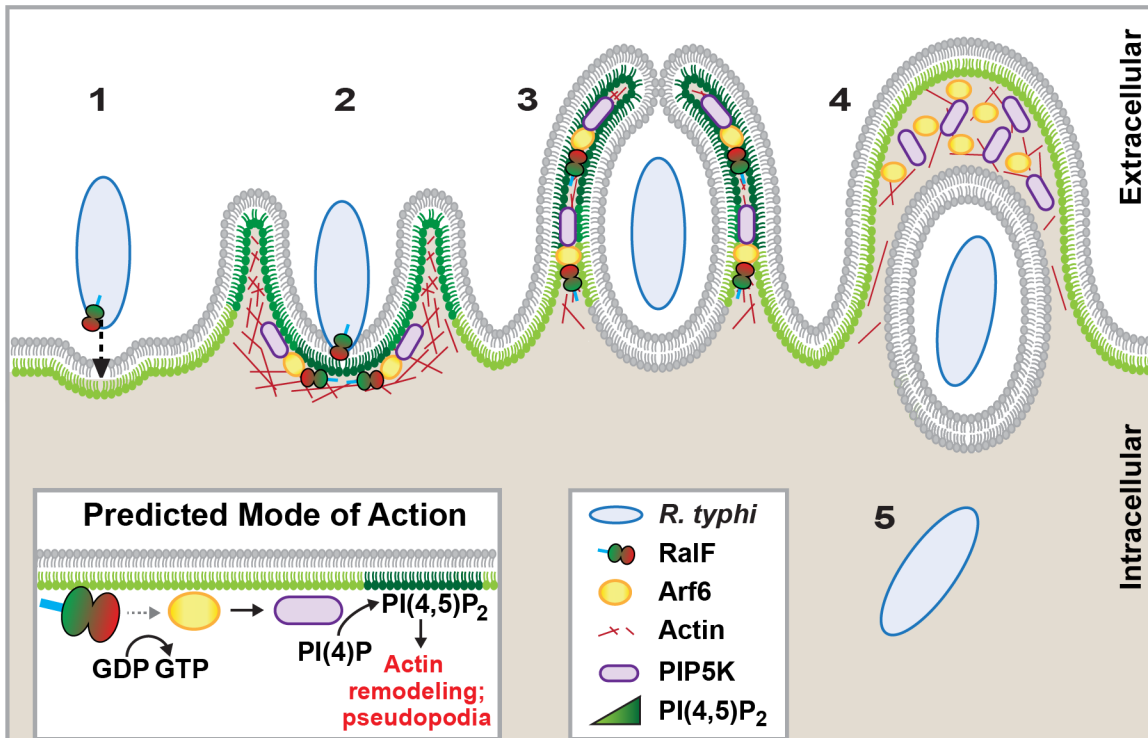


Fig 7. Schematic of *R. typhi* entry. *R. typhi* entry has been broken down into five conceptual stages: binding (1); extension of pseudopodia (2); membrane fusion and internalization (3); formation of early endosome (4); bacterial escape from endosome (5). Schematic is a representation of micrographs from Figs 5B, 5C and 6C. Inset depicts hypothetical recruitment and activation of PIP5K via RalF_{Rt}-activated Arf6, which results in PI(4,5)P₂ enrichment and actin rearrangement to facilitate for *R. typhi* entry.

doi:10.1371/journal.ppat.1005115.g007

Rickettsia species do not reside in vacuoles but rather lyse the phagosome and replicate within the host cytoplasm. Thus, despite carrying a similar Arf-GEF that is unknown from any other bacteria, different intracellular lifestyles across species of *Rickettsia* and *Legionella* have driven divergent roles for RalF during bacterial infection.

Currently, the predominant knowledge of rickettsia entry and invasion of host cells is based on studies of species from SFG rickettsiae, whereby the surface antigen Sca5 binds host receptor Ku70 to activate a signaling cascade leading to Arp2/3 activation and ultimately actin polymerization, membrane rearrangement and bacterial invasion [26,108,109]. The conservation of Sca5 across all *Rickettsia* species implies that this receptor-mediated mechanism for entry is likely conserved (Fig 8) [45]. However, depletion of host Rho family GTPases and nucleation-promoting factors that activate Arp2/3 has only a modest effect on rickettsial invasion, suggesting there are other bacterial or host proteins that activate Arp2/3 during infection [108]. Most species of SFG rickettsiae encode an Arp2/3 activating protein, RickA, which could potentially play this role, although its secretion during infection has yet to be demonstrated. Interestingly, genes encoding RickA are absent from species of TG rickettsiae (*R. typhi* and *R. prowazekii*); thus, if bacterial Arp2/3 activators are a requirement for invasion, factors other than RickA must be utilized for species of TG rickettsiae. Accordingly, we propose that RalF plays a role in host actin rearrangement and bacterial invasion.

Aside from the Sca5-Ku70 interaction and subsequent downstream signaling cascade, other rickettsial adhesins have been characterized for facilitating host cell invasion (Fig 8). However, the lack of conservation of these adhesins (e.g., Sca0 and Sca2) across diverse *Rickettsia* species implies the existence of multiple mechanisms for rickettsial host cell invasion [45]. It is also

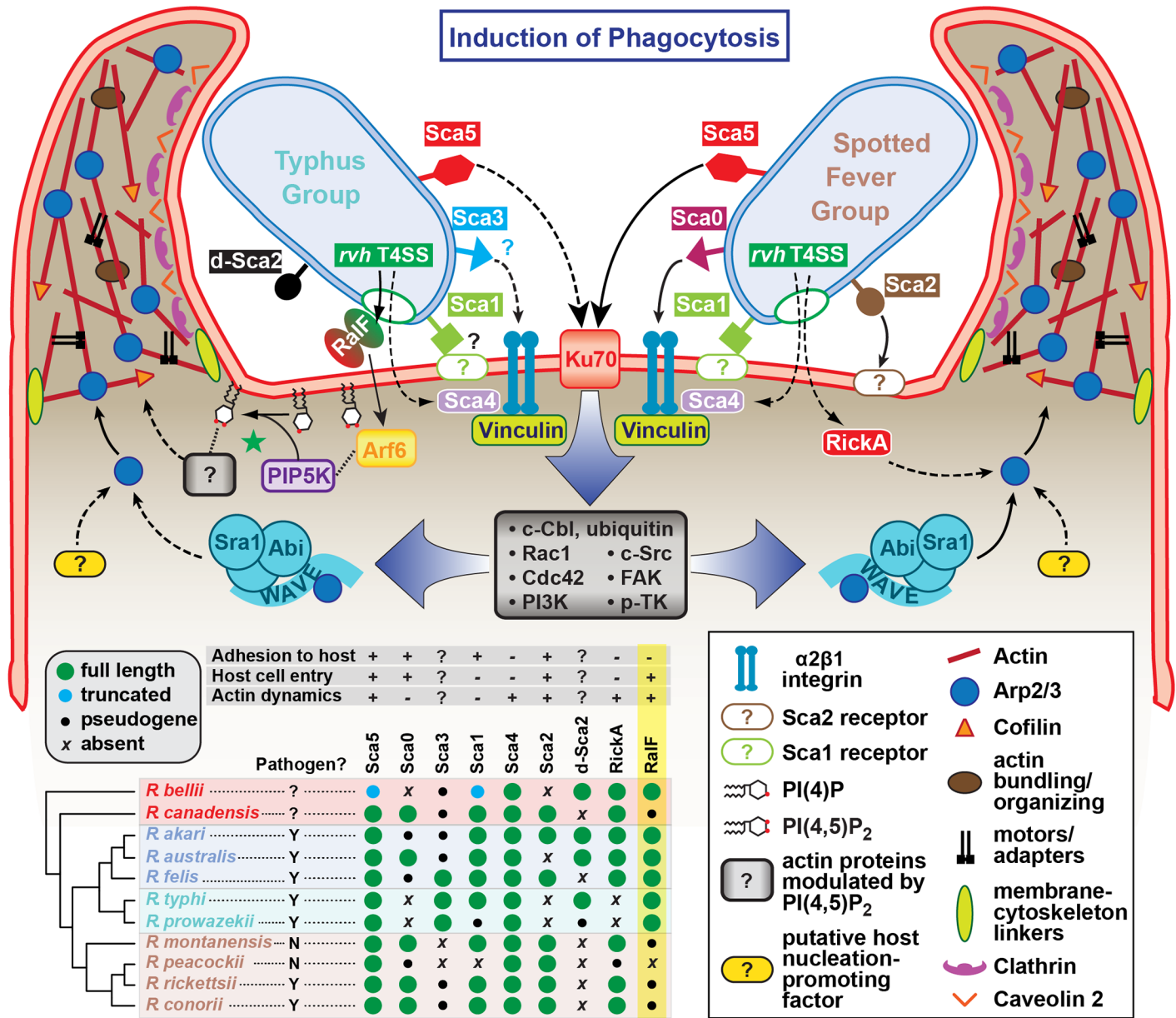


Fig 8. Model for the variable pathways utilized by divergent *Rickettsia* species for host cell entry. General pathways for Typhus Group (TG, left) and Spotted Fever Group (SFG, right) rickettsiae species are inferred primarily from previous work on SFG rickettsiae species *R. conorii* [26] and *R. parkeri* [108] or data from the present study (*R. typhi*). At center, a conserved proximal hub of the pathway commences with Sca5 binding to host receptor Ku70 [110], which triggers a host-signaling cascade (gray box) involving c-Cbl-mediated ubiquitination of Ku70, Rho-family GTPases Cdc42 and Rac1, phosphoinositide 3-kinase (PI3K) activity, and activation of tyrosine kinases (e.g., c-Src, FAK and p-TK) and their phosphorylated targets. The divergent distal arms of this pathway involve recruitment of factors for activating the actin nucleating complex (Arp2/3), which leads to host actin polymerization, extensive membrane ruffling and filopodia formation, and bacterial internalization in a clathrin and calveolin dependent process. For SFG rickettsiae, the WAVE complex recruits Arp2/3, with its activation via an unknown nucleation promoting factor (either host or bacterial; e.g., RickA). While these processes remain to be characterized for TG rickettsiae, our work suggests that secreted RalF recruits the GTPase Arf6, precipitating an accumulation of PI(4,5)P₂ that modulates the activities of a range of actin-associated host proteins (green star). Additional bacterial proteins, some of which are known to facilitate host cell entry, have white lettering with colored boxed backgrounds. Known pathways for protein secretion and host cell receptor-binding, as recently reviewed [45], are shown with solid black lines; all other modeled pathways (shown with dashed lines) are either inferred by homology (e.g., Sca1 of TG rickettsiae as an adhesin based on characterization for Sca1 of *R. conorii* [36]) or estimated based on *in silico* analyses (e.g., Sca3 of TG rickettsiae as a putative analog to the α2β1 integrin-binding Sca0 of *R. conorii* [35]). A phylogenomics analysis across select *Rickettsia* species (bottom, left) illustrates the genomic variation underlying all of the bacterial components of the models. Adapted from our recent report on the *Rickettsia* secretome [45]. Red, ancestral group (AG); blue, transitional group (TRG); aquamarine, TG; brown, SFG.

doi:10.1371/journal.ppat.1005115.g008

probable that each species likely encodes redundancy for factors that facilitate entry, and that some factors may selectively operate for invasion of specific cells (arthropod versus mammalian) throughout the complex rickettsial lifecycle. Thus, it is probable that lineage-specific factors are employed by different species of *Rickettsia* to successfully invade and colonize diverse eukaryotic cells. Our identification of lineage-specific Arf-GEF utilization across diverse rickettsial species exemplifies this, and illuminates previously unappreciated mechanisms for host cell invasion and infection.

Materials and Methods

Bacterial strains, cell culture, and infection

Vero76 (African green monkey kidney, ATCC: CRL-1587), HEK293T and HeLa (ATCC: CCL-2) cells were maintained in minimal Dulbecco's Modified Eagle's Medium (DMEM with 4.5 gram/liter glucose and 480 L-glutamine; Mediatech, Inc.) supplemented with 10% heat inactivated fetal bovine serum (FBS) at 37°C with 5% CO₂. *R. typhi* strain Wilmington (ATCC: VR-144) was propagated in Vero76 cells grown in DMEM supplemented with 5% heat inactivated fetal bovine serum at 34°C with 5% CO₂. Rickettsiae were partially purified as previously described [111]. Infections with *R. typhi* were performed 18–24 hrs post transfection with a multiplicity of infection (MOI) of ~100:1. For antibody pretreatment experiments, partially purified *R. typhi* was incubated with 20 µg Melon Gel IgG (Thermo Scientific) purified rabbit pre-immune serum or anti-RalF_{Rt} polyclonal antibody or 20 µg purified rabbit pre-immune serum or anti-RalF_{Rt} Fab fragments for 30 min prior to infection. Fab fragments were purified using the Fab Purification Kit (Thermo Scientific) according to manufacture's protocol.

Recombinant protein purification and antibody production

The expression and purification of recombinant proteins were performed as previously described [111]. Codon optimized (Life Technologies) *R. typhi* *rvhD4* (RT0284) was cloned into pTrcHis2-TOPO vector under the control of the *trc* promoter (Life Technologies). Full-length *R. typhi* *ralF* was cloned into pEXP5-NT/TOPO (Life Technologies) and transformed into *E. coli* strain bl21-codonplus(de3)-ril (Stratagene). Primers used for cloning can be found in S1 Table. The expression of recombinant proteins was induced with 1 mM IPTG and recombinant proteins were purified by affinity chromatography under native conditions using nickel-nitrilotriacetic acid resin (Ni-NTA) superflow columns (Qiagen) according to manufacturer's instructions. Polyclonal antibody was generated in rabbit using recombinant RalF_{RtFL} (Alpha Diagnostic Intl. Inc).

Bacterial two-hybrid assay

R. typhi gene sequences (RT0362, GenBank accession no. YP_067323) encoding full-length RalF (RalF_{RtFL}) and the *rvh* T4SS signal truncation (RalF_{RtΔT4S}) were cloned into the pTRG "prey" plasmid (BacterioMatch II two-hybrid system; Stratagene). A codon optimized (Life Technologies) *R. typhi* *rvhD4* gene (RT0284, YP_067246) was cloned into the pBT "bait" plasmid. Primers used for cloning can be found in S1 Table. The bait (pBT-RvhD4) and prey (pTRG-RalF_{RtFL} or pTRG-RalF_{RtΔT4S}) plasmids (100ng each) were co-transformed into BacterioMatch II reporter electrocompetent cells according to the manufacturer's instruction (GenePulser Xcell, BioRad). The percent growth of CFUs of reporter cells harboring recombinant plasmids on dual selective screening medium were calculated relative to CFUs obtained on non-selective His dropout medium by a drop plate method for counting CFUs [112].

VirD4 ATPase assay

RvhD4 ATPase activity was monitored using a Quantichrom ATPase/GTPase assay kit (Bioassay Systems), according to the manufacturer's instructions and as described previously [113]. Briefly, 200–12.5 ng/well of purified recombinant RvhD4 protein was incubated in the presence of 1 mM ATP for 30 min at 37°C. Generated free phosphate was quantified by measuring absorbance at OD 620 nm. All of the samples were measured in triplicate wells, and data are given as averages \pm S.D. of three independent experiments.

Protease treatment of *R. typhi*

R. typhi was purified from heavily infected Vero76 cells. Briefly, infected cells were scrapped into media and spun at 12,000 x g for 10 min at 4°C. Cells were resuspended in ice cold PBS, pH 7.2 containing MgCl₂ (PBS-Mg) and sonicated for 10 sec on ice using output 6 of a Sonic Dismembrator (Fisher Scientific). The lysate was filtered through a 5.0 μ m filter (Millipore). The filtrate containing *R. typhi* was layered onto a 20% sucrose cushion at a 1:1 ratio and centrifuged at 16,000 x g for 15 min at 4°C to pellet *R. typhi*. *R. typhi* was resuspended in PBS-Mg and again purified with a 20% sucrose cushion. Purified *R. typhi* was treated with 400 μ g/mL or 800 μ g/mL Proteinase K (Sigma-Aldrich) for 1 hr at room temperature in PBS-Mg buffer as previously described [114]. Following incubation, Halt Protease and Phosphatase Inhibitor Cocktail (Thermo Scientific) was added to the reaction, and bacteria centrifuged at 16,000 x g for 10 min at 4°C. *R. typhi* were washed with PBS-Mg and resuspended in PBS-Mg and NuPAGE LDS sample buffer and reducing reagent (Life Technologies). Lysates were separated on a NuPAGE Bis-Tris SDS-gel (Life Technologies) and immunoblotted with rabbit anti-RalF or anti-EF-Ts as the *R. typhi* cytoplasmic marker [43,115]. Densitometry was performed using ImageJ (NIH) and RalF intensity was normalized to EF-Ts.

Bioinformatics and phylogenomics analyses

Using RalF_{Rt} as a query, BLASTP searches were performed against the NCBI 'Rickettsia' database (taxid:780). Full length RalF_R homologs were aligned with MUSCLE v3.6 [116] using default parameters. Initial domain characterization of RalF_R proteins followed that previously described for *R. prowazekii* [52]. Using Phyre v.2.0 [69], RalF_{Rt} was modeled to the crystal structures of *Legionella pneumophila* RalF (PDB 1XSZ, 4C7P) [50,53] to confirm the boundaries of the Sec7 domain (S7D) and Sec7-capping domain (SCD). The S7D and SCD of *Rickettsia* and *Legionella* RalF homologs were aligned with MUSCLE, superimposing the secondary structure of RalF_L over the alignment.

The divergent C-terminal domain (CTD) of RalF_R proteins was further described based on distinct characteristics, i.e. a sequence of variable length that includes a Pro-rich tract, as well as a putative secretion signal sequence within the terminal 40 aa. Additional *Rickettsia* proteins that lack the S7D and SCD, mostly from SFG rickettsiae, were utilized to characterize this region. All full length and partial RalF_R homologs were used to assess the synteny of the *ralF* locus across select *Rickettsia* genomes. For these genomes, gene neighborhood models were constructed using the Kyoto Encyclopedia of Genes and Genomes (KEGG) database [117], with manual adjustment to gene annotations. Additional bioinformatics/phylogenomics methodologies are described in S2–S5 Figs.

Mammalian expression plasmids and transfections

Genomic DNA from *R. bellii* str. OSU 85–1299, *R. felis* str. Pedreira, *R. montanensis* str. M5/6, and *R. typhi* str. Wilmington was purified using DNeasy Blood and Tissue Kit (Qiagen). RalF

constructs were amplified as EcoRI/BamHI fragments using primers in [S1 Table](#), with the exception of RalF_{RbFL}, which was cloned using Clontech InFusion technology. Amplicons were cloned into the pGEMT-Easy vector (Promega) and confirmed by sequencing (The Biopolymer/Genomics Core Facility, University of Maryland School of Medicine). Plasmids were digested with EcoRI and BamHI, with *ralF* fragments subcloned into the pEYFP-C1 vector (Clontech). All plasmids were transformed into Mix & Go Competent Cells—Strain Zymo 5α (Zymo Research). Plasmids pCDNA3-mRFP-Arf1, pCDNA3-mRFP-Arf5 and pCDNA3-mRFP-P-Arf6 were generous gifts from Prof. Vassilis Koronakis (University of Cambridge, UK). GFP-C1-PLCδ-PH (Addgene plasmid # 21179) was kindly gifted by Tobias Meyer [[118](#)]. All plasmids were purified using PerfectPrep EndoFree Plasmid Maxi Kit (5 Prime).

For transfections, HeLa cells seeded in 8-well chamber slides were transfected with 200ng plasmid per well using Xfect (Clontech) and HEK293T cells in T-75 flasks were transfected with 10μg plasmid using Lipofectamine 2000 (Life Technologies) according to manufactures' protocols.

Immunofluorescence

Twenty-four hours post transfection or at indicated times post infection, cells were fixed with 4% PFA for 10 min at room temperature. Cells were washed three times with PBS and permeabilized in Blocking Buffer (0.2% saponin, 5% FBS in PBS) for 30 min. Primary antibodies mouse anti-PDI (clone RL90, BD Transduction Laboratories, diluted 1:200), mouse anti-GM130 (clone 610822, BD Transduction Laboratories, diluted 1:200), rat anti-*R. typhi* serum (1:500), rabbit anti-RalF_{Rt} (1:100), and rabbit anti-GFP (Life Technologies, diluted 1:1000) were diluted in blocking buffer and incubated with cells for 1 h. Cells were then washed with PBS and incubated with Alexa Fluor 594 or Alexa Fluor 488 secondary antibodies (Life Technologies) diluted 1:2000 in Blocking Buffer for 1 h or 30 min. Finally, cells were washed three times with PBS and mounted using ProLong Gold Anti-Fade mounting media with DAPI (Life Technologies). Actin was stained with Alexa Fluor 594 phalloidin (Life Technologies) and the plasma membrane stained with Alexa Fluor 594 wheat germ agglutinin (WGA, Life Technologies) according to manufacturer's protocol. For confocal microscopy, cells were viewed under a Zeiss LSM 510 Meta Confocal Microscope (University of Maryland Baltimore Confocal Core Facility). For conventional fluorescence microscopy a Nikon Eclipse E600 fluorescent microscope with a Q Imaging Retiga 2000R camera was used to capture images with QCapture Pro software. Images were processed using ImageJ software (NIH). Co-localization analysis was performed using the CoLoc2 plugin in the ImageJ software program [[119](#)]. The Pearson's correlation coefficient was calculated for 5–10 cells per condition from two independent experiments to measure the strength of association between each RalF protein and the cell organelle (i.e., plasma membrane, endoplasmic reticulum, or Golgi apparatus). Two-sided Student's t-tests were performed to determine statistical significance for co-localization coefficients compared to control eYFP.

Cell fractionation

Cellular fractionation was completed as previously described [[52](#)]. Briefly, at 24 hrs post transfection, HEK293T cells were washed once with PBS and collected in 500 μL homogenization buffer (150 mM KCl, 20 mM HEPES pH 7.4, 2 mM EDTA) containing protease inhibitors and passed 30 times through a 27G-needle. The lysate was centrifuged at 2000 x g for 5 min at 4°C to remove the nuclear fraction. The supernatant was subsequently centrifuged at 100,000 x g for 1 h at 4°C to pellet the membrane fraction. The supernatant was removed (cytoplasmic fraction) and the pellet (membrane fraction) was resuspended in 80 μL of homogenization buffer. Twenty micrograms of cytoplasmic and membrane fractions were separated by

SDS-PAGE and blotted with anti-GFP rabbit serum (Life Technologies). Rabbit anti-calnexin [clone ab13505] and mouse anti-GAPDH [clone 6C5] antibodies (Abcam) were used as markers of the membrane and cytosol fractions, respectively.

Ionomycin treatment

Transfected HeLa cells were washed with PBS and incubated in 100 μ L of either phosphate buffered saline (PBS) or Krebs-Ringer solution (120 mM NaCl, 4.7 mM KCl, 1.1 mM CaCl₂, 0.7 mM MgSO₄, 10 mM glucose, 10 mM Na-HEPES, pH 7.4). Ionomycin (Sigma Aldrich) was added to a final concentration of 5 μ M and cells were incubated for 10 min. EGTA was added to a final concentration of 2 mM and cells were incubated for 10 min. Cells were then infected with *R. typhi* (described above) or fixed and stained as described above.

Protein pull-down

RalF_{Rt} was cloned into the pTrcHisA vector (Life Technologies, see [S1 Table](#) for primer sequences) and transformed into Top10 *E. coli* cells (Life Technologies). Protein expression was induced with 1 mM IPTG overnight at 30°C. *E. coli* were lysed using Pierce Lysis Buffer in the presence of HALT Protease Inhibitors (Thermo Scientific) and imidazole added to a final concentration of 10 mM. Lysates were sonicated three times for 20 sec each using setting 6 of a Sonic Dismembrator (Fisher Scientific). mRFP-Arf5 and -Arf6 were expressed in HEK293T cells as described above. HEK293T cells were lysed using Pierce Lysis Buffer in the presence of HALT Protease Inhibitors (Thermo Scientific) and imidazole added to a final concentration of 10 mM.

Pull-down assays were performed using the Pierce Pull-Down PolyHis Protein:Protein Interaction kit according to manufacture's protocol. Briefly, HisPur Cobalt Resin was incubated with rHis-RalF_{Rt} *E. coli* lysate or buffer alone for 1 hr. The resin was washed 5 times and then incubated with either mRFP-Arf5 or -Arf6 HEK293T lysate for 2 hr. Resin was again washed 5 times and bound proteins eluted with 290 mM imidazole elution buffer. Eluted proteins and 10% of the input protein were analyzed by protein immunoblot using the primary antibodies rabbit anti-RalF_{Rt}, rabbit anti-Arf5 (1:1000, Thermo Scientific, PA5-31432) and rabbit anti-Arf6 (1:1000, Thermo Scientific, PA1-093) and the secondary antibody HRP anti-rabbit IgG (1:2000, BioLegend, clone 6B9G9).

Gene knockdown

Negative and MISSION siRNAs against human Arf5 (SASI_Hs01_00024789) and Arf6 (SASI_Hs02_0033275) were obtained from Sigma Aldrich. All siRNA knockdowns were performed in HeLa cells using Lipofectamine 2000 (Life Technologies). Cells were used 24 hrs post transfection. Knockdowns were verified by western blot analysis using 1:1000 dilution of primary antibodies rabbit anti-Arf5 or anti-Arf6 (Thermo Scientific). As a loading control, membranes were re-probed with rabbit anti-GAPDH antibody (1:1000, Abcam).

Data analysis

Graphs show the mean \pm SD of three independent experiments; 100 cells were counted for each condition in every experiment. Statistical analyses were performed using two-tailed equal variance Student's t-test.

Supporting Information

S1 Fig. Qualification of anti-ralF antibody.
(PDF)

S2 Fig. Comparative analysis of the Sec7 domain of RalF proteins from species of *Legionella* and *Rickettsia*.

(PDF)

S3 Fig. Comparative analysis of the Sec7-capping domain of RalF proteins from species of *Legionella* and *Rickettsia*.

(PDF)

S4 Fig. Characteristics of the extended C-terminal domain of *Rickettsia* RalF proteins.

(PDF)

S5 Fig. Genome synteny analysis across the *ralF_R* loci from select *Rickettsia* genomes.

(PDF)

S6 Fig. Densitometry analysis of membrane fractionation.

(PDF)

S7 Fig. Subcellular localization of rickettsial RalF proteins to Golgi apparatus.

(PDF)

S8 Fig. Quantification of rickettsial RalF proteins co-localization with plasma membrane, endoplasmic reticulum and Golgi apparatus.

(PDF)

S9 Fig. Arf1 does not co-localize with RalF_R.

(PDF)

S1 Table. Primers used for this study.

(PDF)

Acknowledgments

We thank Prof. Vassilis Koronakis (University of Cambridge, UK) for plasmids: pCDNA3-mRFP-Arf1, pCDNA3-mRFP-Arf5 and pCDNA3-mRFP-Arf6 and Dr. Tobias Meyer (Stanford University) for plasmid: GFP-C1-PLCδ-PH (Addgene #21179). We are grateful to Dr. Micah Worley (University of Louisville) for generation of the polyclonal anti-RalF_{Rt} antibody. We also thank Susan Rennoll for assistance with graphic artwork.

Author Contributions

Conceived and designed the experiments: KERB MSR JYG AFA. Performed the experiments: KERB MSR JYG MLG SJK SSL. Analyzed the data: KERB MSR JYG SJK. Contributed reagents/materials/analysis tools: MBS AFA. Wrote the paper: KERB MSR JYG MBS AFA.

References

1. Casadevall A. Evolution of intracellular pathogens. *Annu Rev Microbiol.* 2008; 62: 19–33. doi: [10.1146/annurev.micro.61.080706.093305](https://doi.org/10.1146/annurev.micro.61.080706.093305) PMID: [18785836](https://pubmed.ncbi.nlm.nih.gov/18785836/)
2. Hybiske K, Stephens RS. Exit strategies of intracellular pathogens. *Nat Rev Microbiol.* 2008; 6: 99–110. doi: [10.1038/nrmicro1821](https://doi.org/10.1038/nrmicro1821) PMID: [18197167](https://pubmed.ncbi.nlm.nih.gov/18197167/)
3. Kumar Y, Valdivia RH. Leading a sheltered life: intracellular pathogens and maintenance of vacuolar compartments. *Cell Host Microbe.* 2009; 5: 593–601. doi: [10.1016/j.chom.2009.05.014](https://doi.org/10.1016/j.chom.2009.05.014) PMID: [19527886](https://pubmed.ncbi.nlm.nih.gov/19527886/)
4. Creasey EA, Isberg RR. Maintenance of vacuole integrity by bacterial pathogens. *Current Opinion in Microbiology.* 2014. pp. 46–52. doi: [10.1016/j.mib.2013.11.005](https://doi.org/10.1016/j.mib.2013.11.005)

5. Garcia-del Portillo F, Finlay BB. The varied lifestyles of intracellular pathogens within eukaryotic vacuolar compartments. *Trends Microbiol.* 1995; 3: 373–380. PMID: [8564355](#)
6. Ray K, Marteyn B, Sansonetti PJ, Tang CM. Life on the inside: the intracellular lifestyle of cytosolic bacteria. *Nat Rev Microbiol.* 2009; 7: 333–340. doi: [10.1038/nrmicro2112](#) PMID: [19369949](#)
7. Dean P. Functional domains and motifs of bacterial type III effector proteins and their roles in infection. *FEMS Microbiology Reviews.* 2011. pp. 1100–1125. doi: [10.1111/j.1574-6976.2011.00271.x](#) PMID: [21517912](#)
8. Mattoo S, Lee YM, Dixon JE. Interactions of bacterial effector proteins with host proteins. *Current Opinion in Immunology.* 2007. pp. 392–401. PMID: [17662586](#)
9. Hicks SW, Galán JE. Exploitation of eukaryotic subcellular targeting mechanisms by bacterial effectors. *Nat Rev Microbiol.* 2013; 11: 316–26. doi: [10.1038/nrmicro3009](#) PMID: [23588250](#)
10. Galán JE. Common Themes in the Design and Function of Bacterial Effectors. *Cell Host and Microbe.* 2009. pp. 571–579. doi: [10.1016/j.chom.2009.04.008](#) PMID: [19527884](#)
11. Gouin E, Welch MD, Cossart P. Actin-based motility of intracellular pathogens. *Current Opinion in Microbiology.* 2005. pp. 35–45. PMID: [15694855](#)
12. Welch MD, Way M. Arp2/3-mediated actin-based motility: A tail of pathogen abuse. *Cell Host and Microbe.* 2013. pp. 242–255. doi: [10.1016/j.chom.2013.08.011](#) PMID: [24034611](#)
13. Sato H, Frank DW, Hillard CJ, Feix JB, Pankhaniya RR, Moriyama K, et al. The mechanism of action of the *Pseudomonas aeruginosa*-encoded type III cytotoxin, ExoU. *EMBO J.* 2003; 22: 2959–2969. PMID: [12805211](#)
14. Vanrheenen SM, Luo ZQ, O'Connor T, Isberg RR. Members of a *Legionella pneumophila* family of proteins with ExoU (Phospholipase A) active sites are translocated to target cells. *Infect Immun.* 2006; 74: 3597–3606. PMID: [16714592](#)
15. Galán JE, Wolf-Watz H. Protein delivery into eukaryotic cells by type III secretion machines. *Nature.* 2006; 444: 567–573. PMID: [17136086](#)
16. Cascales E, Christie PJ. The versatile bacterial type IV secretion systems. *Nat Rev Microbiol.* 2004/03/24 ed. 2003; 1: 137–149.
17. Backert S, Meyer TF. Type IV secretion systems and their effectors in bacterial pathogenesis. *Current Opinion in Microbiology.* 2006. pp. 207–217. PMID: [16529981](#)
18. Gillespie J, Nordberg E, Azad A, Sobral B. PHYLOGENY AND COMPARATIVE GENOMICS: THE SHIFTING LANDSCAPE IN THE GENOMICS ERA. In: Azad A.F. and Palmer G.H., editor. *Intracellular Pathogens II: Rickettsiales.* Boston: American Society of Microbiology; 2012. pp. 84–141.
19. Walker TS, Winkler HH. Penetration of cultured mouse fibroblasts (L cells) by *Rickettsia prowazeki*. *Infect Immun.* 1978; 22: 200–208. PMID: [215542](#)
20. Walker TS. Rickettsial interactions with human endothelial cells in vitro: Adherence and entry. *Infect Immun.* 1984; 44: 205–210. PMID: [6425214](#)
21. Heinzen RA, Hayes SF, Peacock MG, Hackstadt T. Directional actin polymerization associated with spotted fever group *Rickettsia* infection of Vero cells. *Infect Immun.* 1993; 61: 1926–1935. PMID: [8478082](#)
22. Heinzen RA, Grieshaber SS, Van Kirk LS, Devin CJ. Dynamics of actin-based movement by *Rickettsia rickettsii* in Vero cells. *Infect Immun.* 1999; 67: 4201–4207. PMID: [10417192](#)
23. Van Kirk LS, Hayes SF, Heinzen RA. Ultrastructure of *Rickettsia rickettsii* actin tails and localization of cytoskeletal proteins. *Infect Immun.* 2000; 68: 4706–4713. PMID: [10899876](#)
24. Uchiyama T, Kawano H, Kusuhara Y. The major outer membrane protein rOmpB of spotted fever group rickettsiae functions in the rickettsial adherence to and invasion of Vero cells. *Microbes Infect.* 2006; 8: 801–809. PMID: [16500128](#)
25. Chan YGY, Cardwell MM, Hermanas TM, Uchiyama T, Martinez JJ. Rickettsial outer-membrane protein B (rOmpB) mediates bacterial invasion through Ku70 in an actin, c-Cbl, clathrin and caveolin 2-dependent manner. *Cell Microbiol.* 2009; 11: 629–644. doi: [10.1111/j.1462-5822.2008.01279.x](#) PMID: [19134120](#)
26. Martinez JJ, Seveau S, Veiga E, Matsuyama S, Cossart P. Ku70, a component of DNA-dependent protein kinase, is a mammalian receptor for *Rickettsia conorii*. *Cell.* 2005; 123: 1013–1023. PMID: [16360032](#)
27. Renesto P, Samson L, Ogata H, Azza S, Fourquet P, Gorvel JP, et al. Identification of two putative rickettsial adhesins by proteomic analysis. *Res Microbiol.* 2006; 157: 605–612. PMID: [16574381](#)
28. Vellaiswamy M, Kowalczywska M, Merhej V, Nappez C, Vincentelli R, Renesto P, et al. Characterization of rickettsial adhesin Adr2 belonging to a new group of adhesins in ??-proteobacteria. *Microb Pathog.* 2011; 50: 233–242. doi: [10.1016/j.micpath.2011.01.009](#) PMID: [21288480](#)

29. Park H, Lee JH, Gouin E, Cossart P, Izard T. The rickettsia surface cell antigen 4 applies mimicry to bind to and activate vinculin. *J Biol Chem*. 2011; 286: 35096–103. doi: [10.1074/jbc.M111.263855](https://doi.org/10.1074/jbc.M111.263855) PMID: [21841197](https://pubmed.ncbi.nlm.nih.gov/21841197/)
30. Renesto P, Dehoux P, Gouin E, Touqui L, Cossart P, Raoult D. Identification and characterization of a phospholipase D-superfamily gene in rickettsiae. *J Infect Dis*. 2003; 188: 1276–1283. PMID: [14593584](https://pubmed.ncbi.nlm.nih.gov/14593584/)
31. Radulovic S, Troyer JM, Beier MS, Lau AOT, Azad AF. Identification and molecular analysis of the gene encoding Rickettsia typhi hemolysin. *Infect Immun*. 1999; 67: 6104–6108. PMID: [10531273](https://pubmed.ncbi.nlm.nih.gov/10531273/)
32. Whitworth T, Popov VL, Yu XJ, Walker DH, Bouyer DH. Expression of the Rickettsia prowazekii pld or tlyC gene in Salmonella enterica serovar typhimurium mediates phagosomal escape. *Infect Immun*. 2005; 73: 6668–6673. PMID: [16177343](https://pubmed.ncbi.nlm.nih.gov/16177343/)
33. Rahman MS, Gillespie JJ, Kaur SJ, Sears KT, Ceraul SM, Beier-Sexton M, et al. Rickettsia typhi Possesses Phospholipase A2 Enzymes that Are Involved in Infection of Host Cells. *PLoS Pathog*. 2013; 9. doi: [10.1371/journal.ppat.1003399](https://doi.org/10.1371/journal.ppat.1003399)
34. Li H, Walker DH. rOmpA is a critical protein for the adhesion of Rickettsia rickettsii to host cells. *Microb Pathog*. 1998; 24: 289–298. PMID: [9600861](https://pubmed.ncbi.nlm.nih.gov/9600861/)
35. Hillman RD, Baktash YM, Martinez JJ. OmpA-mediated rickettsial adherence to and invasion of human endothelial cells is dependent upon interaction with $\alpha 5 \beta 1$ integrin. *Cell Microbiol*. 2013; 15: 727–741. doi: [10.1111/cmi.12068](https://doi.org/10.1111/cmi.12068) PMID: [23145974](https://pubmed.ncbi.nlm.nih.gov/23145974/)
36. Riley SP, Goh KC, Hermanas TM, Cardwell MM, Chan YGY, Martinez JJ. The Rickettsia conorii autotransporter protein sca1 promotes adherence to nonphagocytic mammalian cells. *Infect Immun*. 2010; 78: 1895–1904. doi: [10.1128/IAI.01165-09](https://doi.org/10.1128/IAI.01165-09) PMID: [20176791](https://pubmed.ncbi.nlm.nih.gov/20176791/)
37. Cardwell MM, Martinez JJ. The Sca2 autotransporter protein from Rickettsia conorii is sufficient to mediate adherence to and invasion of cultured mammalian cells. *Infect Immun*. 2009; 77: 5272–5280. doi: [10.1128/IAI.00201-09](https://doi.org/10.1128/IAI.00201-09) PMID: [19805531](https://pubmed.ncbi.nlm.nih.gov/19805531/)
38. Cardwell MM, Martinez JJ. Identification and characterization of the mammalian association and actin-nucleating domains in the Rickettsia conorii autotransporter protein, Sca2. *Cell Microbiol*. 2012; 14: 1485–1495. doi: [10.1111/j.1462-5822.2012.01815.x](https://doi.org/10.1111/j.1462-5822.2012.01815.x) PMID: [22612237](https://pubmed.ncbi.nlm.nih.gov/22612237/)
39. Gouin E, Egile C, Dehoux P, Villiers V, Adams J, Gertler F, et al. The Rickettsia conorii activates the Arp2/3 complex. *Nature*. 2004; 427: 457–461. PMID: [14749835](https://pubmed.ncbi.nlm.nih.gov/14749835/)
40. Jeng RL, Goley ED, D'Alessio JA, Chaga OY, Svitkina TM, Borisy GG, et al. A Rickettsia WASP-like protein activates the Arp2/3 complex and mediates actin-based motility. *Cell Microbiol*. 2004; 6: 761–769. doi: [10.1111/j.1462-5822.2004.00402.x](https://doi.org/10.1111/j.1462-5822.2004.00402.x) PMID: [15236643](https://pubmed.ncbi.nlm.nih.gov/15236643/)
41. Kleba B, Clark TR, Lutter EI, Ellison DW, Hackstadt T. Disruption of the Rickettsia rickettsii Sca2 autotransporter inhibits actin-based motility. *Infect Immun*. 2010; 78: 2240–2247. doi: [10.1128/IAI.00100-10](https://doi.org/10.1128/IAI.00100-10) PMID: [20194597](https://pubmed.ncbi.nlm.nih.gov/20194597/)
42. Haglund CM, Choe JE, Skau CT, Kovar DR, Welch MD. Rickettsia Sca2 is a bacterial formin-like mediator of actin-based motility. *Nat Cell Biol*. 2010; 12: 1057–1063. doi: [10.1038/ncb2109](https://doi.org/10.1038/ncb2109) PMID: [20972427](https://pubmed.ncbi.nlm.nih.gov/20972427/)
43. Rahman MS, Ammerman NC, Sears KT, Ceraul SM, Azad AF. Functional characterization of a phospholipase A2 homolog from Rickettsia typhi. *J Bacteriol*. 2010; 192: 3294–3303. doi: [10.1128/JB.00155-10](https://doi.org/10.1128/JB.00155-10) PMID: [20435729](https://pubmed.ncbi.nlm.nih.gov/20435729/)
44. Housley N a, Winkler HH, Audia JP. The Rickettsia prowazekii ExoU homologue possesses phospholipase A1 (PLA1), PLA2, and lyso-PLA2 activities and can function in the absence of any eukaryotic cofactors in vitro. *J Bacteriol*. 2011; 193: 4634–42. doi: [10.1128/JB.00141-11](https://doi.org/10.1128/JB.00141-11) PMID: [21764940](https://pubmed.ncbi.nlm.nih.gov/21764940/)
45. Gillespie JJ, Kaur SJ, Rahman MS, Rennoll-Bankert K, Sears KT, Beier-Sexton M, et al. Secretome of obligate intracellular Rickettsia. *FEMS Microbiol Rev*. 2014; 1–44. doi: [10.1111/1574-6976.12084](https://doi.org/10.1111/1574-6976.12084)
46. Casanova JE. Regulation of Arf activation: the Sec7 family of guanine nucleotide exchange factors. *Traffic*. 2007; 8: 1476–85. doi: [10.1111/j.1600-0854.2007.00634.x](https://doi.org/10.1111/j.1600-0854.2007.00634.x) PMID: [17850229](https://pubmed.ncbi.nlm.nih.gov/17850229/)
47. Cox R, Mason-Gamer RJ, Jackson CL, Segev N. Phylogenetic analysis of Sec7-domain-containing Arf nucleotide exchangers. *Mol Biol Cell*. 2004; 15: 1487–1505. PMID: [14742722](https://pubmed.ncbi.nlm.nih.gov/14742722/)
48. Nagai H, Cambronne ED, Kagan JC, Amor JC, Kahn RA, Roy CR. A C-terminal translocation signal required for Dot/Icm-dependent delivery of the Legionella RalF protein to host cells. *Proc Natl Acad Sci U S A*. 2005; 102: 826–831. doi: [10.1073/pnas.0406239101](https://doi.org/10.1073/pnas.0406239101) PMID: [15613486](https://pubmed.ncbi.nlm.nih.gov/15613486/)
49. Nagai H, Kagan JC, Zhu X, Kahn RA, Roy CR. A bacterial guanine nucleotide exchange factor activates ARF on Legionella phagosomes. *Science*. 2002; 295: 679–682. doi: [10.1126/science.1067025](https://doi.org/10.1126/science.1067025) PMID: [11809974](https://pubmed.ncbi.nlm.nih.gov/11809974/)
50. Amor JC, Swails J, Zhu X, Roy CR, Nagai H, Ingmundson A, et al. The structure of RalF, an ADP-ribosylation factor guanine nucleotide exchange factor from Legionella pneumophila, reveals the

- presence of a cap over the active site. *J Biol Chem.* 2005; 280: 1392–1400. doi: [10.1074/jbc.M410820200](https://doi.org/10.1074/jbc.M410820200) PMID: [15520000](https://pubmed.ncbi.nlm.nih.gov/15520000/)
51. Gillespie JJ, Williams K, Shukla M, Snyder EE, Nordberg EK, Ceraul SM, et al. Rickettsia phylogenomics: unwinding the intricacies of obligate intracellular life. *PLoS One.* 2008; 3: e2018. doi: [10.1371/journal.pone.0002018](https://doi.org/10.1371/journal.pone.0002018) PMID: [19194535](https://pubmed.ncbi.nlm.nih.gov/19194535/)
 52. Alix E, Chesnel L, Bowzard BJ, Tucker AM, Delprato A, Cherfils J, et al. The Capping Domain in RalF Regulates Effector Functions. *PLoS Pathog.* 2012; 8. doi: [10.1371/journal.ppat.1003012](https://doi.org/10.1371/journal.ppat.1003012)
 53. Folly-Klan M, Alix E, Stalder D, Ray P, Duarte L V., Delprato A, et al. A Novel Membrane Sensor Controls the Localization and ArfGEF Activity of Bacterial RalF. *PLoS Pathog.* 2013; 9. doi: [10.1371/journal.ppat.1003747](https://doi.org/10.1371/journal.ppat.1003747)
 54. Paris S, Béraud-Dufour S, Robineau S, Bigay J, Antony B, Chabre M, et al. Role of protein-phospholipid interactions in the activation of ARF1 by the guanine nucleotide exchange factor Arno. *J Biol Chem.* 1997; 272: 22221–22226. doi: [10.1074/jbc.272.35.22221](https://doi.org/10.1074/jbc.272.35.22221) PMID: [9268368](https://pubmed.ncbi.nlm.nih.gov/9268368/)
 55. Bui QT, Golinelli-Cohen MP, Jackson CL. Large Arf1 guanine nucleotide exchange factors: Evolution, domain structure, and roles in membrane trafficking and human disease. *Molecular Genetics and Genomics.* 2009. pp. 329–350. doi: [10.1007/s00438-009-0473-3](https://doi.org/10.1007/s00438-009-0473-3)
 56. Donaldson JG, Jackson CL. ARF family G proteins and their regulators: roles in membrane transport, development and disease. *Nat Rev Mol Cell Biol.* 2011; 12: 362–375. doi: [10.1038/nrm3117](https://doi.org/10.1038/nrm3117) PMID: [21587297](https://pubmed.ncbi.nlm.nih.gov/21587297/)
 57. Aizel K, Biou V, Navaza J, Duarte L V., Campanacci V, Cherfils J, et al. Integrated Conformational and Lipid-Sensing Regulation of Endosomal ArfGEF BRAG2. *PLoS Biol.* 2013; 11. doi: [10.1371/journal.pbio.1001652](https://doi.org/10.1371/journal.pbio.1001652)
 58. Petersen TN, Brunak S, von Heijne G, Nielsen H. SignalP 4.0: discriminating signal peptides from transmembrane regions. *Nat Methods.* 2011; 8: 785–6. doi: [10.1038/nmeth.1701](https://doi.org/10.1038/nmeth.1701) PMID: [21959131](https://pubmed.ncbi.nlm.nih.gov/21959131/)
 59. Krogh A, Larsson B, von Heijne G, Sonnhammer EL. Predicting transmembrane protein topology with a hidden Markov model: application to complete genomes. *J Mol Biol.* 2001; 305: 567–80. doi: [10.1006/jmbi.2000.4315](https://doi.org/10.1006/jmbi.2000.4315) PMID: [11152613](https://pubmed.ncbi.nlm.nih.gov/11152613/)
 60. Berven FS, Flikka K, Jensen HB, Eidhammer I. BOMP: a program to predict integral beta-barrel outer membrane proteins encoded within genomes of Gram-negative bacteria. *Nucleic Acids Res.* 2004; 32: W394–9. PMID: [15215418](https://pubmed.ncbi.nlm.nih.gov/15215418/)
 61. Gillespie JJ, Ammerman NC, Dreher-Lesnick SM, Rahman MS, Worley MJ, Setubal JC, et al. An anomalous type IV secretion system in Rickettsia is evolutionarily conserved. *PLoS One.* 2009; 4: e4833. Available: http://www.ncbi.nlm.nih.gov/entrez/query.fcgi?cmd=Retrieve&db=PubMed&dopt=Citation&list_uids=19279686 doi: [10.1371/journal.pone.0004833](https://doi.org/10.1371/journal.pone.0004833) PMID: [19279686](https://pubmed.ncbi.nlm.nih.gov/19279686/)
 62. Gomis-Rüth FX, Solà M, de la Cruz F, Coll M. Coupling factors in macromolecular type-IV secretion machineries. *Curr Pharm Des.* 2004; 10: 1551–65. PMID: [15134575](https://pubmed.ncbi.nlm.nih.gov/15134575/)
 63. Llosa M, Gomis-Rüth FX, Coll M, de la Cruz Fd F. Bacterial conjugation: a two-step mechanism for DNA transport. *Mol Microbiol.* 2002; 45: 1–8. PMID: [12100543](https://pubmed.ncbi.nlm.nih.gov/12100543/)
 64. Vergunst AC, van Lier MCM, den Dulk-Ras A, Stüve TAG, Ouwehand A, Hooykaas PJJ. Positive charge is an important feature of the C-terminal transport signal of the VirB/D4-translocated proteins of Agrobacterium. *Proc Natl Acad Sci U S A.* 2005; 102: 832–7. doi: [10.1073/pnas.0406241102](https://doi.org/10.1073/pnas.0406241102) PMID: [15644442](https://pubmed.ncbi.nlm.nih.gov/15644442/)
 65. Atmakuri K, Ding Z, Christie PJ. VirE2, a type IV secretion substrate, interacts with the VirD4 transfer protein at cell poles of Agrobacterium tumefaciens. *Mol Microbiol.* 2003; 49: 1699–713. Available: <http://www.pubmedcentral.nih.gov/articlerender.fcgi?artid=3882298&tool=pmcentrez&rendertype=abstract> PMID: [12950931](https://pubmed.ncbi.nlm.nih.gov/12950931/)
 66. Christie PJ, Cascales E. Structural and dynamic properties of bacterial type IV secretion systems (review). *Mol Membr Biol.* 22: 51–61. Available: <http://www.pubmedcentral.nih.gov/articlerender.fcgi?artid=3921681&tool=pmcentrez&rendertype=abstract> PMID: [16092524](https://pubmed.ncbi.nlm.nih.gov/16092524/)
 67. Moncalián G, Cabezón E, Alkorta I, Valle M, Moro F, Valpuesta JM, et al. Characterization of ATP and DNA binding activities of TrwB, the coupling protein essential in plasmid R388 conjugation. *J Biol Chem.* 1999; 274: 36117–24. Available: <http://www.ncbi.nlm.nih.gov/pubmed/10593894> PMID: [10593894](https://pubmed.ncbi.nlm.nih.gov/10593894/)
 68. Sears KT, Ceraul SM, Gillespie JJ, Allen ED, Popov VL, Ammerman NC, et al. Surface proteome analysis and characterization of surface cell antigen (Sca) or autotransporter family of Rickettsia typhi. *PLoS Pathog.* 2012; 8: e1002856. doi: [10.1371/journal.ppat.1002856](https://doi.org/10.1371/journal.ppat.1002856) PMID: [22912578](https://pubmed.ncbi.nlm.nih.gov/22912578/)
 69. Kelley LA, Sternberg MJE. Protein structure prediction on the Web: a case study using the Phyre server. *Nat Protoc.* 2009; 4: 363–371. doi: [10.1038/nprot.2009.2](https://doi.org/10.1038/nprot.2009.2) PMID: [19247286](https://pubmed.ncbi.nlm.nih.gov/19247286/)

70. Kay BK, Williamson MP, Sudol M. The importance of being proline: the interaction of proline-rich motifs in signaling proteins with their cognate domains. *FASEB J*. 2000; 14: 231–41. Available: <http://www.ncbi.nlm.nih.gov/pubmed/10657980> PMID: [10657980](https://pubmed.ncbi.nlm.nih.gov/10657980/)
71. Derrien V, Couillault C, Franco M, Martineau S, Montcourrier P, Houlgatte R, et al. A conserved C-terminal domain of EFA6-family ARF6-guanine nucleotide exchange factors induces lengthening of microvilli-like membrane protrusions. *J Cell Sci*. 2002; 115: 2867–79. Available: <http://www.ncbi.nlm.nih.gov/pubmed/12082148> PMID: [12082148](https://pubmed.ncbi.nlm.nih.gov/12082148/)
72. Franco M, Peters PJ, Boretto J, van Donselaar E, Neri A, D'Souza-Schorey C, et al. EFA6, a sec7 domain-containing exchange factor for ARF6, coordinates membrane recycling and actin cytoskeleton organization. *EMBO J*. EMBO Press; 1999; 18: 1480–91.
73. Ogata H, La Scola B, Audic S, Renesto P, Blanc G, Robert C, et al. Genome sequence of *Rickettsia bellii* illuminates the role of amoebae in gene exchanges between intracellular pathogens. *PLoS Genet*. 2006; 2: e76. doi: [10.1371/journal.pgen.0020076](https://doi.org/10.1371/journal.pgen.0020076) PMID: [16703114](https://pubmed.ncbi.nlm.nih.gov/16703114/)
74. Pizarro-Cerdá J, Kühbacher A, Cossart P. Phosphoinositides and host-pathogen interactions. *Biochim Biophys Acta*. 2014; doi: [10.1016/j.bbali.2014.09.011](https://doi.org/10.1016/j.bbali.2014.09.011)
75. Rhee SG, Bae YS. Regulation of phosphoinositide-specific phospholipase C isozymes. *J Biol Chem*. 1997; 272: 15045–8. Available: <http://www.ncbi.nlm.nih.gov/pubmed/9182519> PMID: [9182519](https://pubmed.ncbi.nlm.nih.gov/9182519/)
76. Várnai P, Balla T. Visualization of phosphoinositides that bind pleckstrin homology domains: calcium- and agonist-induced dynamic changes and relationship to myo-[3H]inositol-labeled phosphoinositide pools. *J Cell Biol*. 1998; 143: 501–10. PMID: [9786958](https://pubmed.ncbi.nlm.nih.gov/9786958/)
77. Stearns T, Willingham MC, Botstein D, Kahn RA. ADP-ribosylation factor is functionally and physically associated with the Golgi complex. *Proc Natl Acad Sci U S A*. 1990; 87: 1238–42. Available: <http://www.pubmedcentral.nih.gov/articlerender.fcgi?artid=53446&tool=pmcentrez&rendertype=abstract> PMID: [2105501](https://pubmed.ncbi.nlm.nih.gov/2105501/)
78. D'Souza-Schorey C, Li G, Colombo MI, Stahl PD. A regulatory role for ARF6 in receptor-mediated endocytosis. *Science*. 1995; 267: 1175–8. Available: <http://www.ncbi.nlm.nih.gov/pubmed/7855600> PMID: [7855600](https://pubmed.ncbi.nlm.nih.gov/7855600/)
79. D'Souza-Schorey C, van Donselaar E, Hsu VW, Yang C, Stahl PD, Peters PJ. ARF6 targets recycling vesicles to the plasma membrane: insights from an ultrastructural investigation. *J Cell Biol*. 1998; 140: 603–16. Available: <http://www.pubmedcentral.nih.gov/articlerender.fcgi?artid=2140168&tool=pmcentrez&rendertype=abstract> PMID: [9456320](https://pubmed.ncbi.nlm.nih.gov/9456320/)
80. Vitale N, Chasserot-Golaz S, Bailly Y, Morinaga N, Frohman MA, Bader M-F. Calcium-regulated exocytosis of dense-core vesicles requires the activation of ADP-ribosylation factor (ARF)6 by ARF nucleotide binding site opener at the plasma membrane. *J Cell Biol*. 2002; 159: 79–89. PMID: [12379803](https://pubmed.ncbi.nlm.nih.gov/12379803/)
81. Radhakrishna H, Donaldson JG. ADP-ribosylation factor 6 regulates a novel plasma membrane recycling pathway. *J Cell Biol*. 1997; 139: 49–61. Available: <http://www.pubmedcentral.nih.gov/articlerender.fcgi?artid=2139810&tool=pmcentrez&rendertype=abstract> PMID: [9314528](https://pubmed.ncbi.nlm.nih.gov/9314528/)
82. Chun J, Shapovalova Z, Dejgaard SY, Presley JF, Melançon P. Characterization of class I and II ADP-ribosylation factors (Arfs) in live cells: GDP-bound class II Arfs associate with the ER-Golgi intermediate compartment independently of GBF1. *Mol Biol Cell*. 2008; 19: 3488–500. doi: [10.1091/mbc.E08-04-0373](https://doi.org/10.1091/mbc.E08-04-0373) PMID: [18524849](https://pubmed.ncbi.nlm.nih.gov/18524849/)
83. Massenbourg D, Han JS, Liyanage M, Patton WA, Rhee SG, Moss J, et al. Activation of rat brain phospholipase D by ADP-ribosylation factors 1,5, and 6: separation of ADP-ribosylation factor-dependent and oleate-dependent enzymes. *Proc Natl Acad Sci U S A*. 1994; 91: 11718–22. Available: <http://www.pubmedcentral.nih.gov/articlerender.fcgi?artid=45303&tool=pmcentrez&rendertype=abstract> PMID: [7972129](https://pubmed.ncbi.nlm.nih.gov/7972129/)
84. Honda A, Nogami M, Yokozeki T, Yamazaki M, Nakamura H, Watanabe H, et al. Phosphatidylinositol 4-phosphate 5-kinase alpha is a downstream effector of the small G protein ARF6 in membrane ruffle formation. *Cell*. 1999; 99: 521–32. Available: <http://www.ncbi.nlm.nih.gov/pubmed/10589680> PMID: [10589680](https://pubmed.ncbi.nlm.nih.gov/10589680/)
85. Stradal TEB, Rottner K, Disanza A, Confalonieri S, Innocenti M, Scita G. Regulation of actin dynamics by WASP and WAVE family proteins. *Trends Cell Biol*. Elsevier; 2004; 14: 303–11. doi: [10.1016/j.tcb.2004.04.007](https://doi.org/10.1016/j.tcb.2004.04.007)
86. Alonso A, García-del Portillo F. Hijacking of eukaryotic functions by intracellular bacterial pathogens. *Int Microbiol*. 2004; 7: 181–91. Available: <http://www.ncbi.nlm.nih.gov/pubmed/15492932> PMID: [15492932](https://pubmed.ncbi.nlm.nih.gov/15492932/)
87. Cossart P, Pizarro-Cerdá J, Lecuit M. Invasion of mammalian cells by *Listeria monocytogenes*: functional mimicry to subvert cellular functions. *Trends Cell Biol*. 2003; 13: 23–31. Available: <http://www.ncbi.nlm.nih.gov/pubmed/12480337> PMID: [12480337](https://pubmed.ncbi.nlm.nih.gov/12480337/)

88. Alrutz MA, Srivastava A, Wong KW, D'Souza-Schorey C, Tang M, Ch'Ng LE, et al. Efficient uptake of *Yersinia pseudotuberculosis* via integrin receptors involves a Rac1-Arp 2/3 pathway that bypasses N-WASP function. *Mol Microbiol.* 2001; 42: 689–703. Available: <http://www.ncbi.nlm.nih.gov/pubmed/11722735> PMID: 11722735
89. Eitel J, Dersch P. The YadA protein of *Yersinia pseudotuberculosis* mediates high-efficiency uptake into human cells under environmental conditions in which invasion is repressed. *Infect Immun.* 2002; 70: 4880–91. Available: <http://www.pubmedcentral.nih.gov/articlerender.fcgi?artid=128239&tool=pmcentrez&rendertype=abstract> PMID: 12183532
90. Hardt WD, Chen LM, Schuebel KE, Bustelo XR, Galán JE. *S. typhimurium* encodes an activator of Rho GTPases that induces membrane ruffling and nuclear responses in host cells. *Cell.* 1998; 93: 815–26. Available: <http://www.ncbi.nlm.nih.gov/pubmed/9630225> PMID: 9630225
91. Gillespie JJ, Brayton KA, Williams KP, Diaz MAQ, Brown WC, Azad AF, et al. Phylogenomics reveals a diverse Rickettsiales type IV secretion system. *Infect Immun.* 2010; 78: 1809–23. doi: [10.1128/IAI.01384-09](https://doi.org/10.1128/IAI.01384-09) PMID: 20176788
92. Niu H, Kozjak-Pavlovic V, Rudel T, Rikihisa Y. *Anaplasma phagocytophilum* Ats-1 is imported into host cell mitochondria and interferes with apoptosis induction. *PLoS Pathog.* 2010; 6: e1000774. doi: [10.1371/journal.ppat.1000774](https://doi.org/10.1371/journal.ppat.1000774) PMID: 20174550
93. Lin M, den Dulk-Ras A, Hooykaas PJJ, Rikihisa Y. *Anaplasma phagocytophilum* Anka secreted by type IV secretion system is tyrosine phosphorylated by Abl-1 to facilitate infection. *Cell Microbiol.* 2007; 9: 2644–57. doi: [10.1111/j.1462-5822.2007.00985.x](https://doi.org/10.1111/j.1462-5822.2007.00985.x) PMID: 17587335
94. Garcia-Garcia JC, Rennoll-Bankert KE, Pelly S, Milstone AM, Dumler JS. Silencing of host cell CYBB gene expression by the nuclear effector Anka of the intracellular pathogen *Anaplasma phagocytophilum*. *Infect Immun.* 2009; 77: 2385–91. doi: [10.1128/IAI.00023-09](https://doi.org/10.1128/IAI.00023-09) PMID: 19307214
95. Lockwood S, Voth DE, Brayton KA, Beare PA, Brown WC, Heinzen RA, et al. Identification of *Anaplasma marginale* type IV secretion system effector proteins. *PLoS One.* 2011; 6: e27724. doi: [10.1371/journal.pone.0027724](https://doi.org/10.1371/journal.pone.0027724) PMID: 22140462
96. Liu H, Bao W, Lin M, Niu H, Rikihisa Y. Ehrlichia type IV secretion effector ECH0825 is translocated to mitochondria and curbs ROS and apoptosis by upregulating host MnSOD. *Cell Microbiol.* 2012; 14: 1037–50. doi: [10.1111/j.1462-5822.2012.01775.x](https://doi.org/10.1111/j.1462-5822.2012.01775.x) PMID: 22348527
97. Schulz F, Horn M. Intracellular bacteria: inside the cellular control center of eukaryotes. *Trends Cell Biol.* 2015; doi: [10.1016/j.tcb.2015.01.002](https://doi.org/10.1016/j.tcb.2015.01.002)
98. Peters PJ, Hsu VW, Ooi CE, Finazzi D, Teal SB, Oorschot V, et al. Overexpression of wild-type and mutant ARF1 and ARF6: distinct perturbations of nonoverlapping membrane compartments. *J Cell Biol.* 1995; 128: 1003–17. Available: <http://www.pubmedcentral.nih.gov/articlerender.fcgi?artid=2120412&tool=pmcentrez&rendertype=abstract> PMID: 7896867
99. Humphreys D, Davidson AC, Hume PJ, Makin LE, Koronakis V. Arf6 coordinates actin assembly through the WAVE complex, a mechanism usurped by *Salmonella* to invade host cells. *Proc Natl Acad Sci U S A.* 2013; 110: 16880–5. doi: [10.1073/pnas.1311680110](https://doi.org/10.1073/pnas.1311680110) PMID: 24085844
100. Wong K-W, Isberg RR. Arf6 and phosphoinositol-4-phosphate-5-kinase activities permit bypass of the Rac1 requirement for beta 1 integrin-mediated bacterial uptake. *J Exp Med.* 2003; 198: 603–14. PMID: 12925676
101. Balañá ME, Niedergang F, Subtil A, Alcover A, Chavrier P, Dautry-Varsat A. ARF6 GTPase controls bacterial invasion by actin remodelling. *J Cell Sci.* 2005; 118: 2201–10. doi: [10.1242/jcs.02351](https://doi.org/10.1242/jcs.02351) PMID: 15897187
102. Higgs HN, Pollard TD. Activation by Cdc42 and PIP(2) of Wiskott-Aldrich syndrome protein (WASP) stimulates actin nucleation by Arp2/3 complex. *J Cell Biol.* 2000; 150: 1311–20. Available: <http://www.pubmedcentral.nih.gov/articlerender.fcgi?artid=2150692&tool=pmcentrez&rendertype=abstract> PMID: 10995437
103. Gilmore AP, Burridge K. Regulation of vinculin binding to talin and actin by phosphatidylinositol-4,5-bisphosphate. *Nature.* 1996; 381: 531–5. doi: [10.1038/381531a0](https://doi.org/10.1038/381531a0) PMID: 8632828
104. Hartwig JH, Kwiatkowski DJ. Actin-binding proteins. *Curr Opin Cell Biol.* 1991; 3: 87–97. doi: [10.1016/0955-0674\(91\)90170-4](https://doi.org/10.1016/0955-0674(91)90170-4) PMID: 1854489
105. Johnson RP, Craig SW. Actin activates a cryptic dimerization potential of the vinculin tail domain. *J Biol Chem.* 2000; 275: 95–105. Available: <http://www.ncbi.nlm.nih.gov/pubmed/10617591> PMID: 10617591
106. Rohatgi R, Ho HY, Kirschner MW. Mechanism of N-WASP activation by CDC42 and phosphatidylinositol 4,5-bisphosphate. *J Cell Biol.* 2000; 150: 1299–310. Available: <http://www.pubmedcentral.nih.gov/articlerender.fcgi?artid=2150699&tool=pmcentrez&rendertype=abstract> PMID: 10995436

107. Ayscough KR. In vivo functions of actin-binding proteins. *Curr Opin Cell Biol.* 1998; 10: 102–111. doi: [10.1016/S0955-0674\(98\)80092-6](https://doi.org/10.1016/S0955-0674(98)80092-6) PMID: [9484601](https://pubmed.ncbi.nlm.nih.gov/9484601/)
108. Reed SCO, Serio AW, Welch MD. Rickettsia parkeri invasion of diverse host cells involves an Arp2/3 complex, WAVE complex and Rho-family GTPase-dependent pathway. *Cell Microbiol.* 2012; 14: 529–45. doi: [10.1111/j.1462-5822.2011.01739.x](https://doi.org/10.1111/j.1462-5822.2011.01739.x) PMID: [22188208](https://pubmed.ncbi.nlm.nih.gov/22188208/)
109. Martinez JJ, Cossart P. Early signaling events involved in the entry of Rickettsia conorii into mammalian cells. *J Cell Sci.* 2004; 117: 5097–106. doi: [10.1242/jcs.01382](https://doi.org/10.1242/jcs.01382) PMID: [15383620](https://pubmed.ncbi.nlm.nih.gov/15383620/)
110. Chan YG-Y, Riley SP, Martinez JJ. Adherence to and invasion of host cells by spotted Fever group rickettsia species. *Front Microbiol.* 2010; 1: 139. doi: [10.3389/fmicb.2010.00139](https://doi.org/10.3389/fmicb.2010.00139) PMID: [21687751](https://pubmed.ncbi.nlm.nih.gov/21687751/)
111. Kaur SJ, Sayeedur Rahman M, Ammerman NC, Beier-Sexton M, Ceraul SM, Gillespie JJ, et al. ToIC-dependent secretion of an ankyrin repeat-containing protein of Rickettsia typhi. *J Bacteriol.* 2012; 194: 4920–4932. doi: [10.1128/JB.00793-12](https://doi.org/10.1128/JB.00793-12) PMID: [22773786](https://pubmed.ncbi.nlm.nih.gov/22773786/)
112. Herigstad B, Hamilton M, Heersink J. How to optimize the drop plate method for enumerating bacteria. *J Microbiol Methods.* 2001; 44: 121–129. doi: [10.1016/S0167-7012\(00\)00241-4](https://doi.org/10.1016/S0167-7012(00)00241-4) PMID: [11165341](https://pubmed.ncbi.nlm.nih.gov/11165341/)
113. Binder M, Eberle F, Seitz S, Mücke N, Hüber CM, Kiani N, et al. Molecular mechanism of signal perception and integration by the innate immune sensor retinoic acid-inducible gene-I (RIG-I). *J Biol Chem.* 2011; 286: 27278–87. doi: [10.1074/jbc.M111.256974](https://doi.org/10.1074/jbc.M111.256974) PMID: [21659521](https://pubmed.ncbi.nlm.nih.gov/21659521/)
114. El-Hage N, Babb K, Carroll JA, Lindstrom N, Fischer ER, Miller JC, et al. Surface exposure and protease insensitivity of Borrelia burgdorferi Erp (OspEF-related) lipoproteins. *Microbiology.* 2001; 147: 821–30. Available: <http://www.ncbi.nlm.nih.gov/pubmed/11283278> PMID: [11283278](https://pubmed.ncbi.nlm.nih.gov/11283278/)
115. Pan X, Lührmann A, Satoh A, Laskowski-Arce MA, Roy CR. Ankyrin repeat proteins comprise a diverse family of bacterial type IV effectors. *Science.* 2008; 320: 1651–4. doi: [10.1126/science.1158160](https://doi.org/10.1126/science.1158160) PMID: [18566289](https://pubmed.ncbi.nlm.nih.gov/18566289/)
116. Edgar RC. MUSCLE: Multiple sequence alignment with high accuracy and high throughput. *Nucleic Acids Res.* 2004; 32: 1792–1797. doi: [10.1093/nar/gkh340](https://doi.org/10.1093/nar/gkh340) PMID: [15034147](https://pubmed.ncbi.nlm.nih.gov/15034147/)
117. Ogata H, Goto S, Sato K, Fujibuchi W, Bono H, Kanehisa M. KEGG: Kyoto encyclopedia of genes and genomes. *Nucleic Acids Research.* 1999. pp. 29–34. doi: [10.1093/nar/27.1.29](https://doi.org/10.1093/nar/27.1.29) PMID: [9847135](https://pubmed.ncbi.nlm.nih.gov/9847135/)
118. Suh B-C, Inoue T, Meyer T, Hille B. Rapid chemically induced changes of PtdIns(4,5)P2 gate KCNQ ion channels. *Science.* 2006; 314: 1454–7. PMID: [16990515](https://pubmed.ncbi.nlm.nih.gov/16990515/)
119. Dunn KW, Kamocka MM, McDonald JH. A practical guide to evaluating colocalization in biological microscopy. *AJP Cell Physiol.* 2011; 300: C723–C742. doi: [10.1152/ajpcell.00462.2010](https://doi.org/10.1152/ajpcell.00462.2010)